CATÓLICA

ESCOLA SUPERIOR DE BIOTECNOLOGIA

PORTO

DEVELOPMENT OF INJECTABLE BIOMIMETIC FORMULATIONS MADE OF NATURAL POLYMERS LOADED WITH FOLIC ACID DERIVATIVES FOR MUSCULOSKELETAL TISSUE ENGINEERING

by

Manuel Luís Medeiros Marques da Silva

November 2018

CATÓLICA
ESCOLA SUPERIOR DE BIOTECNOLOGIA
PORTO

DEVELOPMENT OF INJECTABLE BIOMIMETIC FORMULATIONS MADE OF NATURAL POLYMERS LOADED WITH FOLIC ACID DERIVATIVES FOR MUSCULOSKELETAL TISSUE ENGINEERING

Thesis presented to *Escola Superior de Biotecnologia* of the *Universidade Católica Portuguesa* to fulfill the requirements of Master of Science degree in Biomedical Engineering

by

Manuel Luís Medeiros Marques da Silva

Institute of Polymer Science & Technology, Spanish National Research Council (CSIC), Juan de la Cierva, 3, 28006 Madrid, Spain

Escola Superior de Biotecnologia, Universidade Católica Portuguesa, Rua. Arq Lobão Vital, Apartado 2511, 4201-401 Porto, Portugal

Supervised by:

Dr. Luis Rojo del Olmo; Dra. Blanca Vázquez Lasa; Prof. Ana Leite Oliveira

November 2018

Resumo

As doenças musculoesqueléticas incluem mais de 150 condições relacionadas com o sistema locomotor, sendo as mais comuns são a osteoartrite e a artitre reumatóide. Como atualmente afetam mais de 100 milhões de Europeus e nem todos os tratamentos são eficazes, existe a necessidade de procurar abordagens terapêuticas alternativas. Tendo isto em conta, é importante referir a engenharia de tecidos que estuda a implementação de scaffolds que possuam uma combinação equilibrada de células e moléculas bioativas para alcançar soluções funcionais que promovam a regeneração de novos órgãos e tecidos.

O sucesso das terapias de transplante de células através de injeção é limitado pela capacidade das formulações em permitirem a infiltração de uma suspensão celular de elevada densidade por uma matriz extracelular biomimética formada *in situ* e a capacidade de adicionar moléculas bioativas que possam induzir a regeneração dos tecidos. Normalmente, os fatores de crescimento e diferenciação incorporados nestas formulações degradam-se rapidamente, perdendo a sua atividade. Em alternativa, iões metálicos como o estrôncio são capazes de inibir a atividade dos osteoclastos, promovendo a atividade dos osteoblastos. Devido a estas propriedades, estes iões apresentam potencial para o tratamento de patologias do osso pela via de transplante de células através de injeção. O ácido fólico é uma vitamina hidrossolúvel e tem um papel fundamental em inúmeros processos que garantem uma função saudável no corpo humano. Tendo em conta as características do ácido fólico, o folato de estrôncio representa uma boa alternativa para os fármacos que usam este composto uma vez que não existe preocupação quanto aos efeitos secundários do ácido fólico.

Este trabalho teve como objetivo a síntese e caracterização de derivados de vitamina B com catiões divalentes bioativos para obter folato de estrôncio (SrFO), folato de zinco (ZnFO), folato de manganésio (MnFO) e folato de magnésio (MgFO). A síntese e caracterização de dextrano (Dex) e ácido hialurónico (HA) parcialmente oxidados para a sua avaliação como agentes de reticulação biomiméticos de formulações injetáveis à base de gelatina. E ainda o desenvolvimento e otimização de formulações de hidrogéis injetáveis baseados em agentes de reticulação biomiméticos e derivados de folato bioativos.

Os folatos metálicos (MFO) foram preparados por reação entre o ácido fólico e o respectivo cloreto de metal. A composição e estrutura química foram investigadas por

espectroscopia de raios-X por dispersão em energia (EDS), espectrometria de emissão por plasma (ICP), termogravimetria (TGA), espectroscopia de infravermelho (FTIR) e calorimetria exploratória diferencial (DSC). Os valores de metade da concentração inibitória máxima (IC_{50}) dos MFO e a sua ação biológica em células mesenquimais humanas (hMSC) foram avaliadas por determinação da coloração específica para depósitos de cálcio e glicosaminoglicanos (GACs). Formulações injectáveis contendo SrFO/ZnFO foram preparadas em soluções de tampão fosfato (PBS) a partir de gelatina e de HA ou Dex parcialmente oxidados. O tempo de gelificação a 37 ºC foi determinado por reologia no momento de cruzamente entre o módulo elástico (G') e de perda (G'').

Este trabalho constitui mais um passo na preparação de formulações biomiméticas baseadas em polímeros naturais incorporados com derivados de ácido fólico para aplicações musculoesqueléticas. Estas formulações mostram evidências de possuir propriedades químicas e biológicas desejadas, apresentado características apropriadas para uma aplicação não invasiva, com a vantagem de evitar o uso de fatores de crescimento, que normalmente limitam a sua aplicação em termos clínicos como consequência de problemas indesejados associados à estabilidade e à biodisponibilidade de moléculas de sinalização celular baseadas em proteínas.

Palavras-chave: ácido hialurónico, doenças musculoesqueléticas, estrôncio, zinco, ácido fólico

Abstract

Musculoskeletal diseases include more than 150 conditions that concern the locomotor system and the most common are osteoarthritis and rheumatoid arthritis. As musculoskeletal diseases currently affect more than 100 millions of Europeans and not all treatments are effective, there is a need to search for alternative therapeutic approaches. To adress this problem tissue engineering strategies have been used for the implementation of scaffolds that possess a balanced combination of bioactive cells and molecules to achieve functional solutions that promote the regeneration of new organs and tissues.

The success of injection-based cell transplantation therapies is limited by the capacity of formulations to allow infiltration of a high-density cell suspension within an *in situ* forming biomimetic extracellular matrix and the delivery of bioactive molecules to induce tissue regeneration. Frequently, growth and differentiation factors incorporated into these formulations are rapidly degraded and loss their activity. Alternatively, metal ions such as strontium are able to inhibit the activity of osteoclasts, promoting the activity of osteoblasts. Due to these properties, these ions present potential for the treatment of bone pathologies through cell transplantation by injection. Folic acid is a water soluble vitamin and plays a key role in numerous processes that ensure healthy function in the human body. Regarding the characteristics of folic acid, strontium folate represents a good alternative for drugs that use this compound since there is no concern about the side effects of folic acid.

The main goal of this work is synthesis and characterization of vitamin B derivatives with bioactive divalent cations to obtain strontium folate (SrFO), zinc folate (ZnFO), manganese folate (MnFO), and magnesium folate (MgFO). The synthesis and characterization of partially-oxidized dextran (Dex) and hyaluronic acid (HA) for their evaluation as biomimetic crosslinking agents of gelatin based injectable formulations and the development and optimization of injectable hydrogel formulations based on biomimetic crosslinking agents and bioactive folate derivatives.

The metal folates (MFO) were prepared by hydrothermal reaction between folic acid and the respective metal chloride. Chemical composition and structure were determined by X-ray spectroscopy (EDS), inductively coupled plasma (ICP), thermogravimetric analysis (TGA), fourier transform infrared (FTIR) and differential scanning calorimetry analysis (DSC). Mean inhibitory concentration (IC_{50}) values of MFO

and their biological action on human mesenchymal stem cells (hMSC) were assessed by determination of specific staining for calcium and glycosaminoglycans (GACs) deposition. Injectable formulations bearing SrFO/ZnFO were prepared in phosphate buffered saline (PBS) solutions from gelatin and partially oxidized Dex and HA loaded into a two-component mixing syringe. Gelation time at 37 ºC was determined by rheological oscillatory determination at the time of elastic (G') and loss (G'') moduli crosspoint.

The present developed work constitutes a step forward in the preparation of biomimetic formulations based on natural polymers loaded with folic acid derivatives for musculoskeletal applications. These formulations show appropriate features for their application in non-invasive musculoeskeletal tissue engineering applications, with the advantage of avoiding the use of growth factors that usually limited their transition into clinic as consequence of their undesired problems associated with stability and bioaviability of protein-based cell signaling molecules.

Key-words: hyaluronic acid, musculoskeletal conditions, strontium, zinc, folic acid

Acknowledgments

This Master's thesis constitutes an important step in my life, an end of a period in which I have developed in several aspects. The Catholic University of Portugal, more specifically the Faculty of Biotechnology, represents by distinction the most important and exciting time of my life. This work is the last step of a course, which could only be possible with the contribution and encouragement of some people.

Mainly, I would like to manifest my gratitude to Dr. Luis Rojo del Olmo, who guided me over this dissertation period. For all the support, opinions, wisdom sharing, personal generosity and most of all for the patience and for always pushing me further. I could not wish to have a better mentor than the one I had.

My gratitude also goes to Dra. Blanca Vázquez Lasa for offering me the opportunity of working and be part of the Institute of Polymer Science & Technology Biomaterials research group. For the guidance, total support and availability in helping me with any issue that came during my work.

I would also like to express my gratitude to Prof. Dra. Ana Leite Oliveira for have estabilished the contact with the Biomaterials research group, for the support, knowledge sharing, opinions and for the words of encouragement.

I thank my labmates and all the CSIC's family for having welcomed me so well.

To Josephine and family for welcomed me so well and for all the good experiences during my stay in Madrid.

To my friends for all the moments, conversations, for always believing in me and giving me even greater motivation when I needed.

Finally, a very special thanks to my parents and my brother that always have been by my side during this journey. For their unconditional love and support that helped me being who I am today. I dedicate this work to them.

Contents

List of Figures

List of Tables

List of abbreviations

Dex	Dextran
DSC	Differential scanning calorimetry
ECM	Extracellular matrix
EDS	X-ray spectroscopy
EU	European Union
FTIR	Fourier Transform Infrared
HA	Hyaluronic acid
hMSC	Human mesenchymal stem cells
ICP	Inductively coupled plasma
IPN	Interpenetrating Polymeric Networks
MC	Musculoskeletal conditions
MgFO	Magnesium folate
M_n	Average Number molecular weight
MnFO	Manganese folate
MSC	Mesenchymal stem cells
M_w	Weight number molecular weight
OA	Osteoarthritis
OI	Osteogenesis Imperfecta
OP	Osteoporosis
RA	Rheumatoid arthritis
SEC	Size exclusion chromatography
SrFO	Strontium folate
TGA	Thermogravimetric analysis
TGFβ	Transforming growth factors
XRD	X-ray diffraction
ZnFO	Zinc folate

1. State of the art of Musculoeskeletal Tissue Engineering

1.1. Regenerative medicine: tissue engineering

Tissue engineering and regenerative medicine is a multidisciplinary area of research that includes principles of chemistry, biology, and engineering sciences towards growth, development, and regeneration of damaged tissues or organs. [1] It requires scaffolds with a balanced combination of cells and bioactive molecules to reach functional solutions which promote the design of new organs and tissues.

Considering all tissues in the body, bone is the most broadly investigated for tissue engineering because of its large potential for regeneration. Due to their osteoinductive and osteoconductive characteristics, bone graft materials have been used in order to repair bone fractures and other defects [1]. Despite this use, concern issues are related with the risk of disease transfer, infection, chronic pain, and increase of operative time and cost [1].

Biomaterials that can mimic the structural, mechanical, and biological properties of natural tissues have been given special attention. Good progress has been done regarding the design and the process of new materials in order to produce a successful environment which promotes the capacity of cells to integrate, differentiate and proliferate [2-4]. This is a significant matter once regeneration processes must achieve the desired cell function and stimulate specific cellular responses and activate genes that stimulate cells differentiation and extracellular matrix (ECM) production for enhancing the regeneration of the damaged tissues. Regarding the three-dimensional (3D) nature of the bone, the assistance of a porous and permeable polymeric scaffold that can give a proper environment is crucial to support and regenerate tissues. The 3D polymeric scaffolds provide frameworks for cells to attach, proliferate, and form ECM. Additional bioactive molecules, such as growth factors or their biomimetic functional activators, enzymes and other regulators of cell attachment, proliferation and differentiation, are very appropriate and required in order to improve the regeneration of tissues in a biomimetic approach [2-4].

Natural and synthetic polymers with the specific functionality offer several attractive possibilities for design and development. The combination of microstructural design and preparation of molecular polymer architectures, synthetic pathways and technological methodologies for the preparation of Tissue Engineering scaffolds and drug delivery devices, provides a powerful tool for Regenerative Medicine (Figure 1).

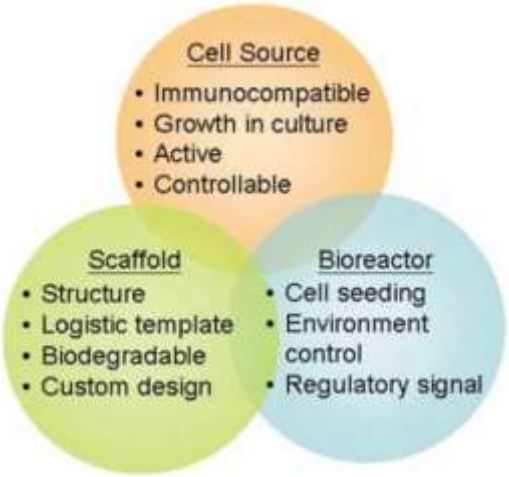

Figure 1- Principal components of the three key pillars supporting the tissue engineering paradigm.

1.2. Musculoskeletal diseases

Musculoskeletal diseases include more than 150 conditions which concern the locomotor system, such as muscles, bones, joints, tendons or ligaments, as listed in the International Classification of Diseases [5]. These diseases vary from those which happens suddenly and for a short period of time like fractures or lifelong condition which are linked with ongoing pain and disability. Musculoskeletal conditions (MC) are the most usual cause of serious hard long-term pain and disability in the European Union (EU) and carry big social support and healthcare costs [5]. They have a relevant economic impact once they are the principal reason of work absence and incapacity leading to productivity loss. Despite the big impact of these conditions on the health and wellbeing of populations in the EU there is a lack of awareness of musculoskeletal conditions. This together with the lack of routinely collected indicators that are specifically important and related to musculoskeletal diseases means that these conditions do not receive yet the attention which is proportionate to the magnitude of their impact [5]. The most common musculoskeletal conditions are osteoarthritis, fractures associated with bone fragility and systemic inflammatory conditions such as rheumatoid arthritis [5], as will be described in this report later.

European population is getting older because of the decreasing of the birth rates and an increasing in life expectancy. Around 2050, it is estimated that the EU population ranged between 15 years old and 64 years old will be decreased in 48 million while the erderly population above 65 will be increased in 58 million people [5]. Thus, risk factor for

musculoskeletal problems related with ageing is becoming asocial challenge to have in consideration by health systems. For instance, a study of the provision of total hip replacement and total knee replacement showed that compared with people aged between 50 and 59 years, those who are between 60 and 84 got more provision relative to need, while those aged above 85 received less total hip replacement and less total knee replacement [6].

In relation to gender, studies have shown that women are more conducive to have MC related diseases than men [7]. Nowadays, MC related diseases affect in a direct way more than 100 million Europeans. Through the 'Bone and Joint Decade' initiative, at the beginning of the millennium, the World Health Organization attributed the high burden of MC related diseases on societies which have an increasingly ageing population [8-9]:

- Almost half of the people over 70 years have osteoarthritis (OA) of the knee.

- Near 80 % of people with OA have some kind of restriction of movement, and one fourth are not capable of doing their normal activities during the day.

Taking these data into account, the challenges and priorities for EU research agenda (H2020) are organized in three distinct points that are excellence in science research, creating industrial leadership and competitive frameworks and tackling societal challenges which focus on addressing the major issues of our society, including age, health and wellbeing [9]. Therefore, the preliminary objectives that were settled down to improve the treatment of musculoskeletal disorders were developing regenerative therapies to enable endogenous healing, tissue-engineered strategies using cell factories, proteins and novel bio-mimetic scaffolds for the treatment of bone, tendon, muscle and cartilage injuries or diseases and novel treatments for surgical repair of bone in an ageing European population. This needs to be based on interdisciplinary cooperation between bone biologists, bioengineers, clinicals, material scientists and industry, and be supported by patient advocates for implementation. To improve pipelines for translation and clinical evaluation, the H2020 will upgrade diagnostics of diseases. This will be done by a mechanism basis such that early treatment strategies effectively enable preventative and early onset strategies for OA, osteoporosis and childhood bone degenerative disorders, such as osteogenesis imperfecta and Paget's disease, among others. To upgrade the clinical systems for delivering high-quality, cost-effective care and monitor effectiveness of outcome, H2020 will make a development and evaluation of new interdisciplinary care models for both treatment and prevention, aiming for major causes of disability such as OA, fragility fractures and spinal disorders [9].

Osteoporosis (OP) is defined as a disease in which lost of bone mass occurs and consequently induces the disruption of bone architecture, causing bone fragility and high fracture risk [5,10,11,12]. Fragility fractures numbers enhance sharply with age. For this reason, the proportion of fractures at any site also varies with age. This is more noticed for hip and forearm [5]. Therefore, the number of fractures and their type are related with the age of the populations at risk. In Portugal, the number of incident fractures in 2010 was estimated at 52000, comprising 10000 hip fractures, 8000 vertebral fractures, 8000 forearm fractures and 26000 other fractures (i.e. fractures of the pelvis, rib, humerus, tibia, fibula, clavicle, and other). It is important to mention that 70 % of fractures occurred in women. When accounting for the demographic projections for 2025, the number of incident fractures was estimated at 69000, representing an increase of 17000 fractures [11] (Figure 2).

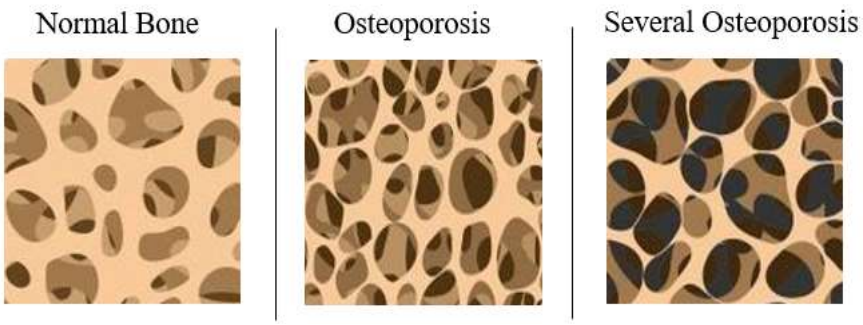

Figure 2- Comparison between a normal bone matrix and one with osteoporosis.

OA is considered as a degenerative disease, which principally has an affect in the articular cartilage [13]. The disease is more common in the joints (continually stressed throughout the years including the knees, hips, fingers and lower spine region) and entails higher disability as the age progresses. The occurrence of osteoarthritis is dificult to predict because of its gradual and slow evolution and consequently the trouble to determine a new case [13]. So, there is limited data about this subject. Taking into account such data that are from developed countries, 10 % of the population above 60 years have clinical problems that can be related to osteoarthritis. For either gender the incidence of this disease increases to people above 50 years and reaches the maximum occurrence between 70 and 79 years. The higher incidence of this disease is in the knee, in both genders.

Rheumatoid arthritis (RA) is classified as a systemic autoimmune disease featured by chronic inflammation of synovial joints resulting in destruction of cartilage and possibly, bone [5,14]. It is the most common inflammatory disease of the joints. It affects 1 % of global's

population with an occurrence ratio of 3 women per men. It normally shows pain, symmetrical swelling and stiffness of the small joints in both hands and feet. This disease causes irreversible damage in bones shape and the joints become deformed, causing a lot of pain and disability. For a study of 100000 cases, depending on the change in the study parameters, the number of people affected varies from 25 to 115 [15]. In Northern European countries, the annual occurrence fluctuates between 20 and 50 cases per 100000 and in the Southern European countries the numbers suggest that the rate of incidence is lower [16,17]. Some research of the occurrence and prevalence of RA show some variations even in populations of the same country. An explication for that kind of results includes diferent variables such as climate, behavioral factors, RA diagnosis, environmental exposure and genetic factors [15].

Osteogenesis Imperfecta (OI) is a genetic disorder in which the bones break easily. People who suffers from this disease present a congenital defect which has a negative effect on the body's ability to produce healthy and functional bones. Harshly affected patients have various fractures since childhood, spontaneous or related to minimal trauma and the children that are more affected could die in the neonatal period [18]. This disease is different from the other ones that were approached in this report because it has a higher incidence in children. OI has a worldwide occurrence rate of 1/15000. The difficulties in the diagnosis, optimal treatment and late developments regarding this disease could became a serious problem for physicians because they can miss diagnosis. OI is characterized by being a hereditary disease due to a collagen defect, mainly caused by mutations of the genes coding the chains of collagen type 1 gene, which leads normally to autosomal dominant OI. Collagen I is the most abundant protein in vertebrates, and is present in large quantities in many connective tissues. Many of the other rare forms of OI are due to defects in protein involved in crosslinking, hydroxylation, and mineralization of type-I collagen [19]. Most patients have a low bone mineral density (BMD), to some extent negatively correlated to clinical severity [20]. Generally, the high fracture incidence observed in children with OI decreases after puberty.

Current clinical therapies differ from each other due to several parameters like efficacy, safety or convenience and should be individualized because the response to the treatment can be different. Taking these into account, some of the therapies that were administrated are described in the Table 1.

Table 1- Examples of current clinical therapies for musculoskeletal diseases.

Bisphosponates	Hormone Therapy
Bisphosphonates are classified as antiresorptive agents that inhibit osteoclast which causes less bone turnover, increasing bone mass and improving mineralization [21]. All bisphosphonates can reduce the risk of vertebral fractures in randomized clinical trials of postmenopausal women with osteoporosis [22-24].	Hormone therapy (estrogen monotherapy) is also responsible to prevent osteoporosis in postmenopausal women, despite the primary indication is for the treatment of menopausal symptoms such as vasomotor symptoms. Therefore, estrogen is capable to reduce the risk for vertebral and hip fracture, as well as the risk of nonvertebral fracture [21].
Strontium Ranelate	**Denosumab**
Strontium Ranelate has a dual effect of reducing bone resorption and increasing bone formation [21]. It is approved for the prevention and treatment of osteoporosis outside of North America [26]. At present the last directive of EMA/235924/2014 European Medicines Agency has put its use under surveillance [27].	Denosumab is a monoclonal antibody appropriate for women at high fracture risk or who have failed other osteoporosis therapies and may be considered in patients with renal insufficiency [21].

As described, current treatments of damaged cartilage and bone tissue include the use of disease-modifying drugs and ultimately surgical intervention due to the limited ability of musculoskeletal tissues to self-regenerate. However, the strategies of tissue engineering for potential future regenerative therapies can become very important to make easier the recruitment of repairing cells and improve musculoskeletal metabolism. These novel treatments consist on acellular scaffolds based on hydrogels and materials which are produced from synthetic polymers such as PLGA and naturally occurring ECM components derived from collagen, glycosaminoglycans (GAG) like hyaluronic acid (HA) and signalling molecules such as transforming growth factors (TGFβ1 and TGFβ3), and bone morphogenetic proteins (BMP-

2) and also have the use of distinct stem cell lineages such as human mesenchymal stem cells (hMSCs) [28–33]. Besides that, powerful treatments for musculoskeletal disorders based on new polymer therapeutics for the controlled delivery of disease-modifying drugs, anti-inflammatory conjugates or inhibitors of matrix metalloproteinases and immunomodulators such as strontium folate [34, 35] or ibuprofen [36] are being performed especially in osteoarthritis and rheumatoid arthritis in which the effectiveness of tissue regeneration is limited by joint inflammation [37]. Regarding the problem of the effectiveness of tissue regeneration is limited by joint inflammation it is important to mention macrophages and their action on these issues. Macrophages are cells of the innate immune system involved in immunological response against pathogens but also in autoimmune disorders such as rheumatic diseases. Macrophage cells release several inflammatory cytokines and chemokines that has a negative effect in cartilage and bone leading to tissue destruction. Macrophages numbers increase enormously in inflammation and in autoimmunity diseases [38,39].

Macrophages can be activated and obtain a phenotype, which varies from proinflammatory (M1) to anti-inflammatory (M2). M1 macrophages are involved in killing microorganisms and tumor cells and are responsible for releasing high amounts of pro-inflammatory cytokines, reactive nitrogen and oxygen intermediates. M2 macrophages are implicated in resolution of inflammation through phagocytosis of apoptotic neutrophils, reduced production of pro-inflammatory cytokines, and increased synthesis of mediators relevant in tissue remodelling [38].

Regarding the different types of macrophages, they can have an important function in diseases like rheumatoid arthritis or osteoarthritis. Inflammation favors expression of M1 macrophages leading to destruction of tissues. On the other hand, in the absence of inflammation M2 macrophages can become activated in order to produce inflammatory cytokines, which leads to the action of enzymes derived from collagen, promoting the regeneration of tissues [39].

1.3. Acellular Scaffolds and cell-laden matrices

The concept of scaffold-based tissue engineering is related to cultivation of isolated cells that come from the patient or donor into a scaffolding system that helps the growth and function of the isolated cells into a specific tissue precursor which could be placed again in the injured site of the patient where tissue regeneration is needed. The main components that can establish the hit of tissue engineering include cells and the matrices/scaffolds. Scaffolds have a very

important role in tissue engineering because they can give structural support for the cells to accommodate and guide their growth in the 3D space into a specific tissue or organ.

Therefore, it is important to refer current bone tissue engineering strategies like acellular scaffolds and cell-laden matrices. The first ones can be prepared from two different ways: one is to manufacture artificial scaffolds and the other one is to withdraw cellular components from tissues using chemical and mechanical manipulations to make collagen-rich matrices [40]. These matrices have slow degradation and are usually substituted by the ECM proteins secreted by the ingrowing cells. The main target of a process of decellularization is to take away all cellular material without any consequences to the ECM. Acellular tissues matrices have shown to have the ability to support cell ingrowth and regeneration of genitourinary tissues with no evidence of immunogenic rejection [40]. To have success in tissue engineering it is very important to choose the right scaffold. Despite of several biodegradable polymer scaffolds that have been developed, acellular scaffolds have some advantages such as the capacity to retain their correct anatomical structure even after the decellularization process, the ability to maintain the native ECM architecture and the decellularization process facilitates similar biomechanical properties as those of native tissues that are critical for the long-term functionality of the grafts.

On other hand, cell-laden matrices are defined as a scaffold that encapsulates cells inside their cross-linked polymer network structure to mimic the native tissue-like structure and function [41]. Cell-laden hydrogels are the most recent option as carriers to deliver cells into a certain site within the body. Cells encapsulating hydrogels could be used for the generation of 3D tissue engineering structures. Studies showed that the cell-laden hydrogels constitute a good solution for cell seeding, oxygen delivery and mass transfer in large 3D cell and tissue engineering. The methods usually used for 3D cell-culture are cell spheroids, microspheres and *in situ* forming hydrogels [41]. Due to the several merits associated with cell-laden hydrogels in terms of structure and functions that mimics the native ECM, these kinds of hydrogels have applications in different areas such as tissue engineering, drug delivery and gene delivery. Although cell-laden hydrogels are well established and proven to be useful, there are still a few challenges to build tissue constructs with biomimetic architecture and function. In addition, cellular rearrangement within cell-laden scaffolds often does not resemble the biomimetic structure of the native tissue, which hinders proper cell microenvironment interactions, cell phenotype preservation and cell differentiation (Figure 3) [42].

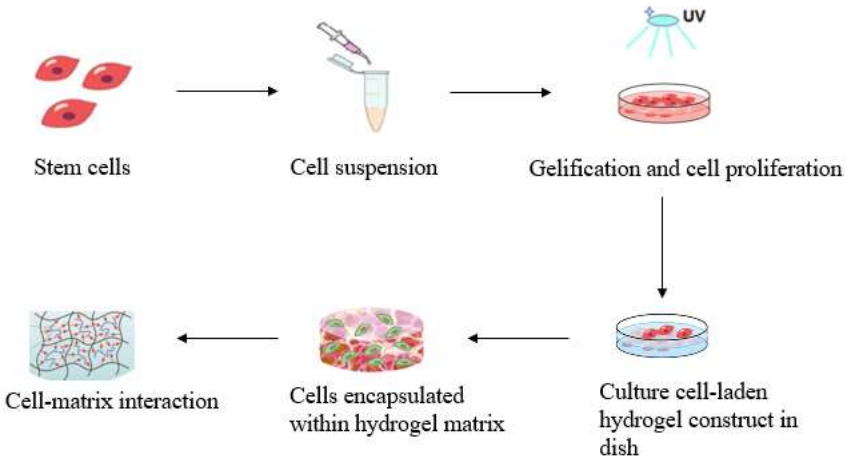

Figure 3- Schematic diagram representating the fabrication of cell-laden hydrogels [41].

1.4. Stem cells: osteoblasts and osteoclasts

The cells that are responsible for bone formation are the osteoblasts. They originate from bone marrow mesenchymal stem cells (MSCs), which can also give rise to chondrocytes, fibroblasts, and adipocites, among others. The compromise of mesenchymal cells to the osteoblastic lineage depends on the specific activation of transcription factors induced by morphogenetic and developmental proteins that carry out the functions of bone matrix protein secretion and bone mineralization. After bone matrix formation different things can hapen to mature osteoblasts. Some of them remain entrapped in bone and turn into osteocytes, some become flat to cover bone surfaces and most die by apoptosis [43]. The major role of osteoblasts is to synthesise collagen type I and other matrix proteins that could be used to model for mineral deposition in the form of hydroxyapatite. Mature osteoblasts that are very involved in this process are recognized by their location on the bone surface. Osteoblasts express high levels of alkaline phosphatase and the concentration of this protein in blood reflects the rate of bone formation [43].

Osteoclasts are the only cells capable of bone resorbing. They are extremely important in healthy bone development and remodelling. Bone turnover and some diseases can be a result of dysfunction of osteoclasts results. They are intimately associated with the surface of bone [44].

Osteoblasts and osteoclasts operate in cooperation and an imbalance may result in a variety of diseases, including osteoporosis. Osteoblasts regulate osteoclasts via the receptor activator of nuclear factor κ-B ligand (RANKL)-receptor activator of nuclear factor κ-B

(RANK) signalling pathway. It binds the receptor RANK, which is produced on osteoclasts and their progenitors. The interaction of RANK with RANKL is required for osteoclast formation, differentiation, activation and survival. RANKL-RANK signalling is important in the osteoblast regulation of osteoclasts [45]. Osteoprotegerin and soluble RANK have been developed as pharmaceutical candidates [46], and anti-human RANKL neutralizing antibody (denosumab) has gained approval from the Food and Drug Administration and the European Medicines Agency for the treatment of postmenopausal osteoporosis and cancer-associated bone disorders [47].

Stem cells are unspecialized cells, capable of renewing themselves for long periods without relevant changes in their properties. Stem cells can differentiate into various multi-lineage cells under certain physiological or experimental conditions [48]. Due to their potential in clinical applications, stem cells became an important subject in modern research era. Considering the homing ability, multilineage potential, secretion of anti-inflammatory molecules and immunoregulatory effects, MSCs are considered as promising cell source for treatment of autoimmune, inflammatory and degenerative diseases such as RA [48]. In preclinical studies on animal models, MSCs were found to be helpful in RA recovery and decreasing disease progression [48].

1.5. Extracellular Matrix (ECM)

The composition and architecture of the ECM dictates the physical, chemical and mechanical properties of all body tissues and also provides support. ECM is the microenvironment of cells. Specific signalling molecules are responsible for cells communication and for that reason that molecules also regulates ECM behavior. ECM show a very dynamic structure and also participates in cell activities, such as cell proliferation, adhesion, migration, and differentiation. The major constituents of ECM are fibrous proteins with a support function (collagens, fibronectin, elastin), other specific proteins (growth factors, small integrin-binding glycoproteins), proteoglycans and water [49]. ECM faces up a continuous remodelling done by cells that cleave, rearrange, and deposit the distinct components and set the tissue architecture, with mutual interactions. All cells are in connection with their ECM, either continuously or at certain significant stage of their life [50]. The mechanism of ECM maintenance is complex and the process of remodelling allows adjustment of stem cell diferentiation and it is vital during growth and wound healing. Furthermore, anomalous ECM dynamics create a deregulation of cell activities, resulting in congenital defects that can guide into pathological tissue growths (fibrosis and cancer). Understanding the

remodelling mechanisms of ECM is very important from the point of view of tissue engineering and regenerative medicine [51]. Moreover, ECM serves as storage for molecules and growth factors, transmits and distributes the loads preventing mechanical failure, partitions and distributes cells in specific functional units [52].

ECM is a very high hydrated macromolecular network composed by some proteins and proteoglycans (PGs). Almost all the proteins are glycoproteins [53], characterized by oligosaccharide chains covalently attached. PGs are glycoproteins but consist of big clusters of carbohydrate chains, GAGs, attached to a core protein. Inside the GAGs, exists HA that does not have a protein component.

1.6. Natural and Synthetic Polymers

HA is a natural linear polysaccharide formed by repeating units of D-glucuronic acid and N-acetyl-D-glucosamine disaccharide [54]. It is one of the mains constituents of the ECM and can be found in almost all the body [54]. HA has a function in some biological processes, such as cell growth, migration and differentiation [54]. HA shows good properties for application in the biomedical field, because it is a biocompatible, biodegradable, nontoxic, non-immunogenic polymer with high water affinity and presents multiple possibilites of chemical modifications including multiple acid and hydroxyl groups [54]. This constituent of the ECM has been showing a range of different applications from tissue scaffolds to cosmetic materials [54]. For instance, in the biomedical field, HA has to date been used mainly to prepare scaffolds for tissue engineering and drug delivery systems (Figure 4) [54].

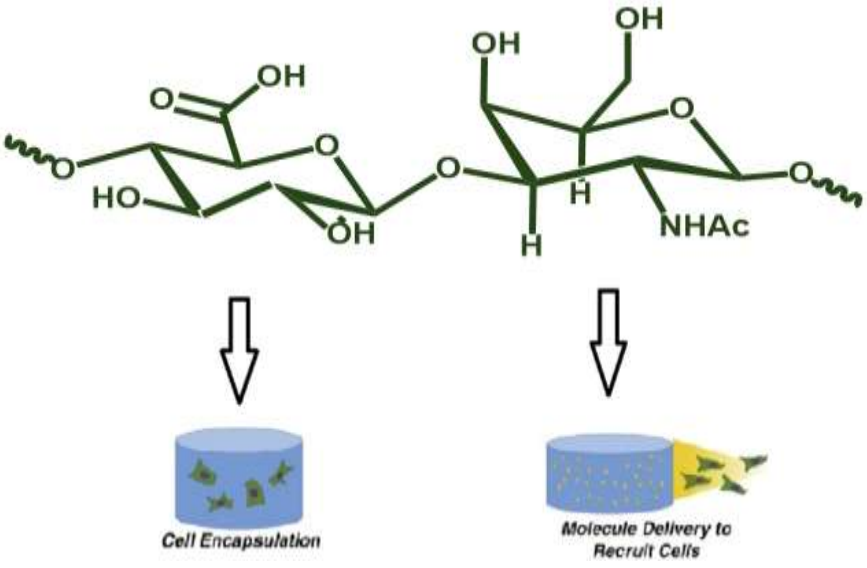

Figure 4- Chemical structure of HA and applications [55].

Dextran (Dex) is also classified as a natural polymer. Cross-linked dextran hydrogels are recognized to provide propitious ECM conditions due to high water content and good biocompatibility. Yet, some of the disadvantages of these hydrogels are related with not satisfactory mechanical properties. These structures are prone to deformation which limits their use in hard tissue engineering applications [56]. However, dextran has a very high amount of hydroxyl functional groups that makes it suitable to do chemical modifications [57].

Collagen is protein that exists in higher quantities in the human body and is the dominant ECM constituent of most tissues. Collagen is not only primarily related with cells and tissues structural support but also has an important function on cellular behavior and chemokine storage and release [58]. The collagen building block is a right-handed triple helix of three polypeptide α chains, held together in the core by hydrogen bonding. The α chains that make up the triple helix generally follows a tripeptide repeating unit of G-X-Y where G is glycine, X is often proline, and Y is often hydroxyproline or hydroxylysine. When assembled into the triple helix building block, the glycine residues face in toward the helix core and the proline in the second position allows the polypeptide chain to twist [59,60]. It is thought that at least 25 different types of collagen exist [59]. The amino acid compositions of the α chains determines the type of collagen. Of all the collagen types, types I and II are most abundant in the human body [61].

Gelatin is a commonly used natural polymer that is derived from collagen, where the hydrogen bonds between the triple helix α chains have been broken. Gelatin has similar biocompatibility but reduced mechanical properties and faster degradation than collagen [62]. It is highly soluble in aqueous solutions and forms a thermally reversible hydrogel. Gelatin can also be used to produce three-dimensional porous scaffolds [63]. Many times, it is associated with other natural polymer to upgrade the biological activity of the scaffold [64,65]. Like collagen, gelatin is crosslinked with glutaraldehyde to raise the mechanical stiffness and increase degradation time [66]. Gelatin sponges, and powders, are clinically used as haemostatic agents. Taking into account where the gelatin products are applied, complete resorption of material can happen between two days and six weeks [67].

Scaffolds for tissue engineering have a critical role regarding the regeneration of tissues and organs. Therefore, there are two classes of polymer materials for biodegradable scaffold fabrication: synthetic and natural [68].

Synthetic polymers can offer innumerable chances for the preparation of porous systems, controlled degradable matrices and modulated scaffolds for tissue engineering and drug delivery. The choose of monomeric species and the advanced possibilities of new synthetic ways have opened a large perspective for the preparation of polymer systems with specific properties. The macromolecular chemistry has a significant function in the design and preparation of systems with specific structures, morphologies and properties. So, for the preparation of synthetic polymers are used molecules that give high molecular weight polymers, functionality, structural order and orientation, nano and micro-crystallinity, and modulated biodegradability [68].

Again, natural polymers when compared to synthetic are advantageous due to the fact that they resemble the protein and polysaccharide extracellular matrix components. Cells recognize and possess the necessary binding domains for the amino acid and saccharide sequences. The elastomeric backbone of synthetic polymers usually needs surface changes or chemical functionalization to be able to make selective cell binding. Given the strict regulatory standards for material purity and consistent quality, scaffold materials should have controllable and reproducible properties. Consequentially, the lack of batch-to-batch reproducibility in material properties and quality assurance/quality control (QA/QC) manufacturing practices are currently challenging to implement in natural polymers. In contrast, synthetic polymer material properties are reproducible from batch-to-batch because they are determined by tunable processing parameters and the QA/QC practices are well established [68].

For the preparation of tissue engineering scaffolds, it is essential an equilibrium between hydrophilic/hydrophobic character. Relatively to soft tissue healing, the majority of the scaffolds are based on hydrophilic polymers because they have the ability to form very defined 3D matrices that mimic the microstructure and properties of ECM [69,70]. For that reason, cell population can experiment a proper environment and stimulation, which increases their physical integration on highly hydrated body environments such as musculoskeletal, myocardium, and other soft tissues [71,72,73]. Hydrophilic synthetic polymers including amides, esters, ethers, phosphates, and urethanes can be yield in high quantities with particular structures and molecular weights offering better control of the chemical composition and matrix architecture than natural polymers [74]. But ideal and perfect hydrophilic matrices do not exist. Instead a huge amount of polymeric families can be synthesized to suit into the desired properties of the tissue to be restored. Generally, these properties can be achieved through modifications regarding the functionality of the macromolecular chains with impact in the

chemical structure [70]. The polar component of the free energy of the surface of synthetic polymeric based scaffolds can be enhanced due to the fact that some derived functional groups such as amino, amide, carbonyl or phosphorous are present, which renders the biomedical devices more susceptible to adsorption of adhesion mediated ECM biomolecules [75]. So, very hydrated scaffolds are commonly made from injectable formulations based on hydrophilic synthetic polymers which have the capacity to self-generate hydrogels by physical or chemical crosslinking mechanisms and the synthetic polymers most used for this purpose are poly(glycolic acid) (PGA), poly(ethylene glycol) (PEG), poly(hydroxyethyl methacrylate) (PHEMA), poly(aminoamides) (PAA), poly(aminoacids) [76,77].

1.7. Hydrogels

Hydrogels are a special kind of structures consisting in 3-D hydrophilic, cross-linked polymeric networks capable of absorbing a significant amount of water or biological fluids. Hydrogels have a huge biocompatibility, identical structure to the natural ECM, and tunable physical and biochemical properties, and for that reason have been chosen for many applications in the biomedical field [78]. These water-swollen polymeric cross-linked network can facilitate the adhesion, migration, proliferation, and differentiation of chondrocytes and osteoprogenitor cells to osteoblasts, and deliver effectively substances like nutrients and growth factors [79-83]. The interest around injectable hydrogels which can be formed *in situ* after being injected into the body is rising over the last years [84,85]. After injection the gel formation gives better advantages over normal hydrogels: an injectable matrix can be implanted in the body in an almost non-invasive way and is able to acquire any intended form, to combine with any irregular shaped defects [78, 80]. Therefore, solutions of polymers which can be crosslinked automatically under mild conditions are attracting a great deal of interest. In these systems, crosslinking can occur through physical interactions which may originate by changes in pH, temperature, ionic concentration or through chemical reactions, like Michael addition or Schiff base [78, 84, 86, 87].

Regarding the production of hydrogels, some studies have shown the potential of some natural polymers hydrogels for the delivery of cells and possible bone regeneration.

Ben-David et al. (2011) estabilished a comparison between bone formation in-duced by gelatin alone or in combination with cells cultured under normal or osteoge-nic

conditions at a nude mouse calvarial. The osteogenic cell-laden scaffold induced higher bone formation, indicating continuing cell viability and the persistence of the osteogenic phenotype within the gel. Ratanavaraporn et al. (2012) described increased bone formation with lactoferrin and tritolide released from gelatin in vivo [88].

Also, promising results regarding possible bone regeneration were reported by natural polymers based hydrogels. Bergman et al. (2008) reported the formation of HA-based gels using an aldehyde–hydrazide reaction. Both aldehyde HA and polyvinyl alcohol were modified to incorporate a hydrazide group. These solutions could then be injected from separate syringes, undergoing in situ gelation mediated by reaction of the aldehyde and hydrazide groups to originate stable hydrazine bonds [88]. Kim et al. (2010) manipulated the degradation rate of HA through incorporation of metalloproteinase (MMP)-sensitive peptide sequences. MMP-sensitive HA showed higher bone formation when compared with HA insensitive to MMP degradation [88]. The fabrication of sintering-free composite scaffolds based on biphasic calcium phosphate and chitosan, containing high solids loading in the absence of any other processing additives were established by C.F. Marques et al. [89]. The obtained 3D scaffolds revealed an early and fast drug release, showing a new method for local bone regeneration and infection treatments, once this more direct administration of drug could improve the results when compared to the conventional treatment strategies [89].

Such as hydrogels, Interpenetrating Polymeric Networks (IPNs) and semi-IPN have been tried for potential therapeutic applications and standout as an innovative biomaterial-based structure for drug delivery and as scaffolds for cell cultures. An IPN is achieved when a second hydrogel network is polymerized within a pre-polymerized hydrogel. This is obtained by immersion of a pre-polymerized hydrogel into a solution containing monomers and a polymerization initiatior. IPNs can be formed in two ways. One is by being in the presence of a cross linker in order to generate a full IPN and the second one is in the absence of a cross-linking mechanism to produce a network of embedded linear polymers within the original hydrogel giving rise to semi-IPN. These networks most often show physical-chemical properties that can remarkably differ from those of the macromolecular constituents. Importantly, the network properties can be adapted by the type of polymer and its concentration, by the applied crosslinking method as well as by the overall procedure used for their preparation. In many cases, polysaccharides are selected

for the formation of IPN, semi-IPN, dual network or just single hydrogel networks (Figure 5), which are either chemically or physically crosslinked [57, 90].

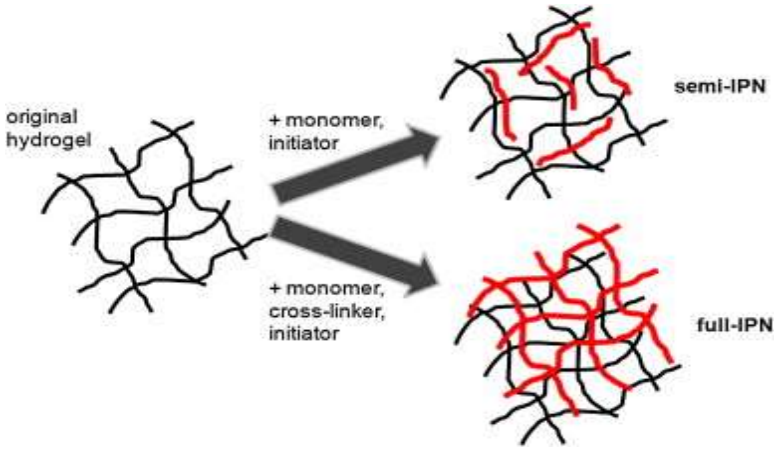

Figure 5- Formation and structure of semi and interpenetrating polymer networks. Reproduced with permission from Elservier ® [91].

1.8. Growth factors, vitamins and ions

Growth factors are promising therapeutic proteins that have the capacity to modulate morphogenetic behaviors, including cell survival, proliferation and differentiation. Among them, some vitamins and ions have also this ability. Growth factors are a group of soluble signalling molecules that can induce cellular division, growth, and differentiation by means of specific binding of transmembrane receptors on target cells. Regarding the biologics involved in cartilage repair, growth factors continue to be the most studied molecules because of their good proliferative, proanabolic or anticatabolic properties [92]. These include select members of the transforming growth factor-β (TGF-β) superfamily, fibroblast growth factor (FGF) family, and insulin-like growth factor-1 (IGF-1) [93,94].

The TGF-β family has over 30 structurally related members and plays a relevant function in the regulation of embryogenesis as well as adult homeostasis [92,95]. TGF-β1, 2, and 3 are seen as good stimulators of chondrogenesis, since their application increases the production of cartilaginous ECM in bone marrow-derived MSCs as well as stimulates synthetic activity in chondrocytes and also induces Sox9 expression [94,96,97]. TGF-βs are very expressed during MSC condensation in the first stages of cartilage repair and also in the growth plate of long bones for animal models [98,99]. Therefore, TGF-β1 and 3 have been selected to be used in some in vivo studies investigating the capacity of TGF-βs to induce the restore of cartilage defects [92]. For instance, in a rabbit full thickness cartilage defect model, poly(lactic-

co-glycolicacid) / fibrin gel scaffolds loaded with MSCs and TGF-β1 had better results in promoting the cartilage reparation when compared to those loaded only with MSCs [100]. However, the effects of TGF-β1 on cartilage repair *in vivo* are not consistent, showing also some negative effects. Some reasons have been proposed for the observed negative effects of TGF-β delivery, among wich stands out the relatively non-specific effects of TGF-β on MSC differentiation [101]. For that reason, it is relevant to take into account the quantity of TGF-βs when delivered *in vivo* and know that TGF-βs are multifunctional and induce different gene responses in distinct cell types for regarding proliferation and ECM synthesis [102].

Folic acid belongs to a group of water-soluble vitamins, which contain B-group vitamins and is needed to ensure healthy function of numerous processes of the human body including the role of a co-enzyme in the normal DNA synthesis, and also acts as part of the co-enzyme system in amino acid and nucleoprotein synthesis [103]. Folic acid is an excellent targeting vehicle in drug delivery [104].

It is proved that zinc (Zn) is a fundamental cofactor for enzymes involved in protein synthesis like bone matrix components, DNA and RNA and also is one main component of the cell membrane repair machinery and musculoskeletal matrix regeneration [105]. Zn has two major functions related to bone biology. It has a structural role in the bone matrix and it is implicated in the preservation of bone mass once it stimulates bone formation by osteoblasts and inhibits bone resorption by osteoclasts [106]. Besides, it has been demonstrated that deficient Zn intake or a defect in the absorption of it can lead to growth and gonadal development retardation [107,108]. Moreover, Zn also has a significant role in cartilage matrix metabolism, cartilage II and SOX9 gene expression and inflammatory-related diseases carried out by Zn-dependent matrix metalloproteinases (MMPs) [109–112].

More than half of the magnesium (Mg) stored in the human body is in the bone. Mg is fundamental to all living cells, including, for instance, osteoblasts and osteoclasts. Intracellularly, Mg is essential for various physiological processes. It is fundamental for ATP synthesis, the principal source of energy in the cells [113]. Besides, Mg is a cofactor of innumerous enzymes involved in nucleic acid, lipid and protein synthesis [113]. Also, due to its positive charge, Mg has a role regarding stabilization of cell membranes and functions as a signal transducer [114]. For that reason, changes in Mg homeostasis has a direct effect on cell and tissue functions. Regarding some studies about different species, dietary Mg restriction

induces osteoporosis [115] since the number of osteoblasts detected is reduced [116,117] and an increment in the number of osteoclasts has been described [115].

Manganese (Mn) has an important role regarding the metabolism of muscle and bone [118] and can be found in some tissues and organs like the bone, liver or pancreas. It is reported that Mn is a fundamental cofactor of enzymes for cell functions, like arginase, RNApolymerase, pyruvate carboxylase and superoxide dismutases [119,120]. Moreover, Mn^{2+} ions appears to be the more efficients acting as activators of various glycoproteins that are important for some cellular events like cellular adhesion and proliferation as well as mediating interactions between cells and the ECM [118,121–124]. Prolidase is a cytosolic imidodipeptidase, which specifically splits imidodipeptides with C-terminal proline or hydroxyproline. The enzyme plays an important role in the remodeling of bone tissue, releasing their essential components, showing that has a specific requirement for manganese [120]. Besides, it is reported that this element has a relevant function in keeping bone mass, once its decrease has a negative impact patients with osteoporosis [118,125,126].

In recent years was discovered that strontium (Sr) had a good impact on bone metabolism. Strontium ions have been found to inhibit osteoclast activity, while promoting osteoblast activity, which facilitates bone formation [127]. Meanwhile it has been hypothesised that the strontium cation also has a function in the inhibition of osteoclast differentiation and the activity is mediated by the increase in osteoprotegerin markers and the decrease in the RANK ligand. As was previously said, the process of bone formation is substantially handled by some systemic and *in situ* biological agents. Strontium is recognized that has a good impact on hMSC differentiation, bone formation and remodelling ability *in vivo* [127] by a two connected ways, concretely the decrease of osteoblast activity and the increase of osteoclast activity and that fact is the major reason why it has reccently started to be used for treatment of osteoporosis during the last times, mainly in the form of complexes with organic acids such as ranelic acid via oral administration (Figure 6) [128].

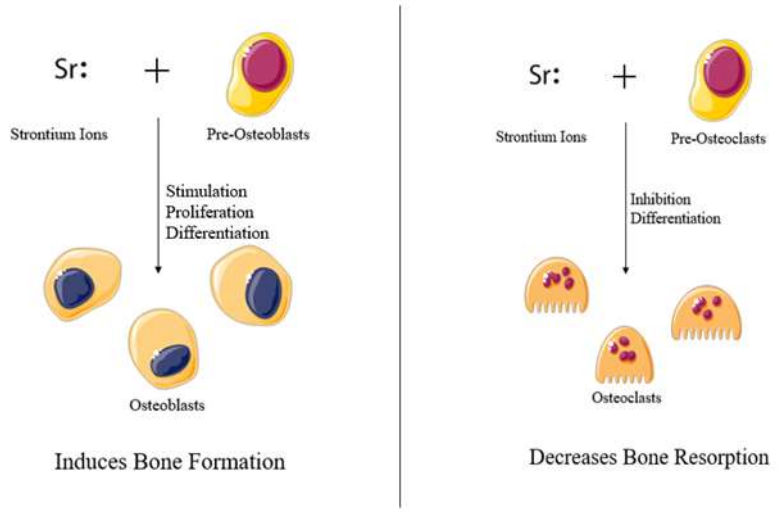

Figure 6- Biological action of strontium on osteoblast and osteoclast differentiation and the effect on bone methabolism [129].

Therefore, a controlled local release of strontium is the most desirable administration way in order to surpass some of the disadvantages linking with the methods of systemic administration that existed until now [128]. Strontium folate has been recently studied and represents a promising alternative to current strontium bearing drugs with no concerning about the pharmacological effects of the vitamin-B derivative contra-ion [128]. It also has advantages on cell replication and differentiation processes and allows cellular proliferation and colonization of missing tissues, therefore promoting full regeneration of critical bone defects where the damage is large enough to prevent proper healing [128].

Since Sr and Zn cations do not suffer degradation reactions during processing, storage and transport, there is an important research activity developing promising alternatives in the application of these compounds as bioactive agents in musculoskeletal regenerative therapies. Due to that reason, of the four elements approached in this report, Sr and Zn will be the ones studied more broadly.

2. Objectives

The main goal of this work is the development of semi-interpenetrating hydrogels based on hyaluronic acid, dextran, gelatin and osteoinductive compounds such as strontium or zinc and to study their properties towards applications on biomedical field, especially in the treatment of muskuloskeletal diseases. With this purpose the following objectives are considered:

- Synthesis and characterization of vitamin B derivatives with bioactive divalent cations to obtain strontium folate (SrFO), zinc folate (ZnFO), manganese folate (MnFO), and magnesium folate (MgFO).
- Synthesis and characterization of partially-oxidized dextran and hyaluronic acid for their evaluation as biomimetic crosslinking agents of gelatin based injectable formulations.
- Development and optimization of injectable hydrogel formulations based on biomimetic crosslinking agents and bioactive folate derivatives.

3. Materials and Methods

Four complexes of acid folic were synthesized and formulated into hydrogels based on dextran and hyaluronic acid. This section describes the reagents, procedures and the characterization techniques used for this purpose.

3.1. Reagents

Materials used in this work were suplied from commertial sources**:** gelatin pharmaceutical degree (100 %) with molecular weight of 50 KDa from Reinert-Gruppe Ingredients, hyaluronic acid (98 %) with molecular weight of 400 KDa from Stanford Chemicals, folic acid (97 %) from Alfa Aesar, magnesium chloride hexahydrate (99 %) from Merck, strontium chloride hexahydrate (99%) from Acros Organics, zinc chloride (99 %) from Fluka Analytical, manganese chloride (97%) from Alfa Aesar, dextran pharmaceutical degree (100 %) with molecular weight of 70 KDa and sodium periodate (99,8 %) from Sigma Aldrich. The remaining chemicals used were obtained from Sigma Aldrich in an analytical grade and used without further purification.

3.2. Methods

3.2.1. Partial Oxidation of Polysaccharides – Dextran 70 and Hyaluronic Acid

A solution of 0.1 g/mL of dextran 70 was dissolved in Milli-Q water. Afterwards a solution of 0.06 g/mL of $NaIO_4$ was added smoothly. The reaction mixture was stirred in the dark for 4 h at room temperature. The solution was then quenched by mixing with a solution containing 0.32 mL of ethylene glycol, for 1h. At the end of the reaction, the solution was dialyzed (molecular weight cut-off = 3.5 kDa) against 1.5 L of Milli-Q water each day for 4 days, lyophilized and stored at room temperature. An analog procedure was used for the partial oxidation of hyaluronic acid. The aldehyde contents of both polysaccharides samples were quantified by the hydroxylamine titration method described below [130].

The percentage oxidation of oxidized HA and dex was quantified by measuring the mol of aldehydes in the polymers through the hydroxylamine method described below. A 0.25 N hydroxylamine hydrochloride solution was prepared containing methyl orange indicator. For this purpose, 8.750 g of hydroxylamine hydrochloride are dissolved in 100 mL of distilled water to which 3.0 mL of methyl orange (0.05% w/v) were added. The solution was then diluted to a

volume of 0.5 L. Then the pH was adjusted to 4.0 with NaOH 1 M. The solution become orange [130]. The method is based on the following reaction:

$$\mathrm{DexHA} + \mathrm{NH_3OH \cdot HCl} \rightarrow \mathrm{DexO \cdot NH_2^{\cdot}OH} + \mathrm{HCl}$$

$$\mathrm{HCl} + \mathrm{NaOH} \rightarrow \mathrm{NaCl} + \mathrm{H_2O}$$

Where the aldehyde groups reacts with the hydroxylamine leading to the production of a Schiff base and HCl for each aldehyde residue. The HCl reacts with the NaOH in a standard titration. The preparation of the samples is based on dissolving 0.100 g of each sample in 25 mL of the solution of hydroxylamine. Each mixture is allowed to stand for 2h. The solutions are titrated with standardized sodium hydroxide solution (0.1145M) until the mixture turn into light salmon colour [130]. The % of aldehydes in the sample is calculated through the following equation:

$$\%\mathrm{Aldehydes} = \frac{(\mathrm{V_{(NaOH)}} \times \mathrm{M_{(NaOH)}})}{(\frac{\mathrm{m_{sample}}}{\mathrm{M_{(HA)}}})} \times 100$$

3.2.2. Synthesis of Srontium, Zinc, Magnesium and Manganese folates

Strontium folate salt was obtained from folic acid and strontium chloride solutions following a described methodology [32]. Briefly, 25 mL of folic acid aqueous solution (0.01M) was prepared and pH adjusted to 7.4 with NaOH (1 M), the solution was then refluxed at 50 ºC for 2 h. Subsequently, 25 mL of a $SrCl_2 \cdot 6H_2O$ solution (1.2 M) in ethanol–H_2O (50 % v/v) were added and the reaction mixture was stirred and heated at 80 ºC for a further period of 1 h. The reaction was quenched by cooling down the mixture in an ice bath and the precipitate formed was collected by filtration. The dark orange solid product was recrystallized twice in hot water, milled and dried at 50 ºC under vacuum until constant weight to be obtain in the form of fine orange crystals.

Analog procedures were adopted for the preparation of new folate complexes based on zinc, magnesium and manganese folate that yielded fine dark orange crystals.

3.2.3. Synthesis of Gels

A phosphate buffered reaction medium containing monobasic potassium phosphate (0.004M) and disodium phosphate (0.02M) was prepared and pH adjusted to 7.4. Then three different kind of gels were prepared maintaining a fixed final volume (1 mL) but different

composition according with Table 2. Each formulation was supplemented with 0.20 mg/mL of strontium folate or 0.12 mg/mL of zinc folate. The time of the addition of the different components with the gelatin dictated the beginning of the gelling reaction. Immediately after mixing the two components, they were placed in a 37 ºC thermostatised bath for 45 minutes.

Table 2- Composition of the different formulations. Buffer pH=7.4 (0.025M Na+K salts)

Formulation Code	Component A (mg/mL)	Component B (mg/mL)		Final Volume (mL)
	Gelatin	HA-ox	Dex-ox	
F1	100	-	100	1
F2		40	-	

3.3. Characterization Techniques

The content of strontium, zinc, magnesium and manganese in the folate complexes was determined by emission spectroscopy analysis using an inductively coupled plasma (ICP) optical emission spectrometer (Perkin-Elmer 430DV).

The experimental metal content for each derivative were obtained by the following equation:

$$\text{Metal}_{(\text{At\%})} = \frac{\text{MM}_{(\text{X})}}{\text{MM}_{(\text{XFO}\cdot\text{NH}_2\text{O})}} \times 100$$

Where X refers to the compounds (Sr, Zn, Mg and Mn) and N represents the number of water molecules for each component.

The absence of halide impurities and crystal composition where confirmed by energy-dispersive X-ray spectroscopy (EDS), recorded on a Hitachi SU8000, and X-ray diffraction (XRD) diffractograms were recorded on a Bruker D8 Advance instrument that works with CuKα radiation at a 0.02 step size and at 0.5 seconds per step.

Coordination mode and chemical composition of folate derivatives and modified HA and dextran were determined by FTIR spectroscopy on a PerkinElmer Spectrum Two spectrophotometer with an ATR attachment.

Average Number (M_n) and weight (M_w) and polidispersity index (PI = M_n/M_w) were determined by size exclusion chromatography (SEC) using a Shimadzu modular system comprising a DGU-20A3 solvent degasser, a LC-20AD pump, column oven, a SIL-20A HT autosampler and a RID-10A refractive index detector. Samples were dissolved (2 mg/mL) in the mobile phase based on Milli-Q water with 0.2 M $NaNO_3$, 0.01M $NaHPO_4$.

Melting points (T_m) of the folate derivatives were measured by differential scanning calorimetry (DSC, Perkin-Elmer DSC 8500). Samples (10 mg) were placed in aluminium pans and heated under a nitrogen flow (20 mL/min) from 30 ºC to 120 ºC at a constant rate of 40 ºC/min and then heated from 120 ºC to 400 ºC at a constant rate of 10 ºC/min. The T_m was taken as the onset of the heat capacity transition observed. Thermogravimetric diagrams were obtained using a thermogravimetric analyser TGA Q500 (TA instruments) apparatus, under dynamic nitrogen at a heating rate of 10 ºC/min in a range of 40–600 ºC.

The experimental water content for each derivative were obtained by the following equation:

$$\text{Metal}_{(H_2O\%)} = \frac{MM_{(NH_2O)}}{MM_{(XFO\cdot NH_2O)}} \times 100$$

Where X refers to the compounds (Sr, Zn, Mg and Mn) and N represents the number of water molecules for each component.

Yield is the amount of product obtained in a chemical reaction. The percentage yield measures the effectiveness of a synthetic procedure. It is calculated by dividing the amount of the obtained desired product by the theoretical amount as represented in the following equation:

$$\text{Yield } (\%) = \frac{\text{mass obtained}}{\text{calculated mass}} \times 100$$

3.4. Rheology Measures

Rheological behaviors of HA/Dex-based hydrogels were analyzed with a Rotational Rheometer Gemini (Bohlin Instruments). The evolution of the storage (G') and the loss (G'') moduli at constant frequency was recorded as a function of the reaction time (time sweep). The gelation process occurred on a parallel cone-plate (diameter 40 mm) under the conditions of a time sweep at 25 ºC, with a 150 μm gap at constant frequency (1 Hz) and amplitude sweep at

0.01–1 Pa. The volume of the samples was 1.0 mL. The assay was performed as shown in Table 3.

Table 3- Rheological assay performed and respective settings.

Test Settings						
Assay	Geometry	Ramp	Sample Points	Temperature (ºC)	Sample Volume (mL)	Rheometer Gap (µm)
Oscillatory Sweep	40 mm parallel plate	Increase shear rate from 0.01 Pa to 1 Pa	251	25	1	150

In total, 12 samples were analyzed in the rheometer at one selected time, as can be seen in Table 4.

Table 4- Samples formulation for rheology tests.

Gel Formulation	Measurement Time
	28 minutes
F1+Sr^{2+}	3 samples
F1+Zn^{2+}	3 samples
F2+Sr^{2+}	3 samples
F2+Zn^{2+}	3 samples

3.5. Releasing Profile of Sr^{2+}, Zn^{2+} and Folic Acid

The amount of folic acid released at 37 ºC for each gel was determined from a calibration curve made from the absorbance of a series of standard solutions of folic acid in a phosphate buffered reaction medium (pH=7.4 (0.025M Na+K salts)) with a concentration range of 5 µg/L

to 100 μg/L (R^2=0.99). Basically, either Sr^{2+} or Zn^{2+} loaded hydrogels were placed into 1 mL of phosphate buffered reaction medium. At the specific selected times, 100 μL samples of the phosphate buffered reaction medium were withdrawn and replaced by 100 μL fresh phosphate medium. The samples were prepared in triplicate and the absorbances of the supernatant were registered at 2 h, 4 h, 24 h, 4 days, 7 days and 14 days, using the equipment NanoDrop Thermo Fisher SpectrumONE ®.

The quantification of Sr^{2+} and Zn^{2+} is carried out by determining the content of these elements in the above supernatant using an ICP plasma-induced atomic emission spectrometer (Perkin-Elmer 430DV) taking as emission wavelength 407.771 nm for the Sr^{2+} and 206.200 nm for Zn^{2+}. The samples were prepared in triplicate and the absorbances of the supernatant were registered at 2 h, 4 h, 24 h, 4 days, 7 days and 14 days.

3.6. Cell/Material Cytotoxicity

Cell culture studies were performed using hMSC (P10576 Innoprot) cells. The culture medium was Dulbecco's modified Eagle's medium - low glucose enriched with 110 mg/L of sodium bicarbonate (DMEM, D5546 Sigma) and supplemented with 20 vol % of fetal bovine serum (FBS, Gibco), 200 mM L-glutamine, 100 units/mL penicillin and 100 mg/mL streptomycin. Cultures were maintained at 37 ºC in humidified air with 5 vol % CO_2, and the culture medium was carefully replaced at selected time intervals under sterile conditions. The cytotoxicity of the samples was assessed by AB (BIO-RAD BUF012B) assay.

Cells (passage 4) were seeded in a sterile 96-well culture plate at a density of 10^5 cells/mL in complete medium (MSCM, P60115, Innoprot) and incubated to confluence for 24 h. Afterward 100 μL of each dilution (0; 0,03; 0,0625; 0,125; 0,25; 0,5 mg/mL) of the folates were added (n= 8) and incubated for 24 h. Non-treated negative controls were used for the calculation of 100% cell viability. After that time, the medium was removed and 100 μL of AB solution prepared in warm DEMEM-low glucose phenol red-free (D4947 SIGMA) (10 % v/v) were added to each well and the plates were incubated at 37 ºC for 3 h. Fluorescence was measured at 590 nm after excitation at 560 nm using a microplate reader (Synergy HT).

Regarding the data of optical densities obtained, the values of the percentages of relative cellular viability (RCV) were obtained through the following equation:

$$\mathrm{RCV}(\%) = \frac{\mathrm{OD_M} - \mathrm{OD_W}}{\mathrm{OD_N}} \times 100$$

Where OD_M, OD_W and OD_N are the optical density measurements of the sample, the blank (media introduced into wells without cells) and the negative control, respectively. In order to calculate the mean inhibitory concentration IC_{50}, a concentration curve is constructed against relative cell viability. The concentration that produces the death of 50 % of the cells present in the negative control is defined as mean inhibitory concentration, IC_{50}. This concentration is the parameter usually used to quantify the toxicity of a drug.

3.7. Cell Viability and Calcium Deposition

HMSCs (passage 2) were seeded in 48 well plates at a density of 10^4 cells per well and cultured for four days in Dulbecco's modified Eagle´'s medium - low glucose enriched with 110 mg/L of sodium bicarbonate (DMEM, D5546 Sigma). Control cultures were used without the presence of folic acid derivatives. Other cultures were prepared in the presence of folic acid derivatives.

Acridine orange (3,6-dimethylaminoacridine) and propidium iodide (5-[3 (diethylmethylammonio)propyl]-6-phenyl-, diiodide) OA/PI were used for stain nuclei. AO and PI are used to accurately determine cell viability. Both AO and PI are fluorescent nuclear probes that can detect viable, apoptotic, and necrotic cells. AO can permeate both live cells and will stain all nucleated cells to generate green fluorescence. PI can permeate cells with poor membrane integrity and will stain all dead nucleate cells to generate red fluorescence. Both AO and PI stain late apoptotic cells with orange nuclei [131,132]. Briefly, hMSC cells on the surfaces were fixed for 15 min with 3.7 % formaldehyde, permeabilised for 10 min with 0.1 % Triton X-100 and stained for 40 min with a 0.5 g/mL OA/PI solution in PBS. Samples were washed with PBS and Tween20 0.1 % and PBS. Images were acquired using a fluorescent microscope (excitation 465/495 nm emission 515/555 nm) Nikon Elipse TE2000-S.

Calcium deposition was qualitatively determined by Alizarin Red staining assay. Briefly, hMSC cells on the well surfaces were fixed for 15 min with 3.7 % formaldehyde and stained for 20 min with 0.5 mL of Alizarin Red 40 nM solution in dH_2O (18MΩ-cm). Samples were washed with dH_2O and dried for direct image analysis using an optical microscope Nikon Elipse TE2000-S.

4. Results and Discussion

4.1. EDS Spectra of Folic Acid Derivatives

The synthetic procedure for producing strontium, zinc, magnesium and manganese based folate complexes from chlorine salts are expected to provide fewer impurities than hydroxide or carbonate derivatives and no other co-precipitates [33]. Accordingly, EDS analysis exhibits the presence of expected elements with no significant impurities as shown in Figure 7. The four folates were obtained in high yields (> 95 %).

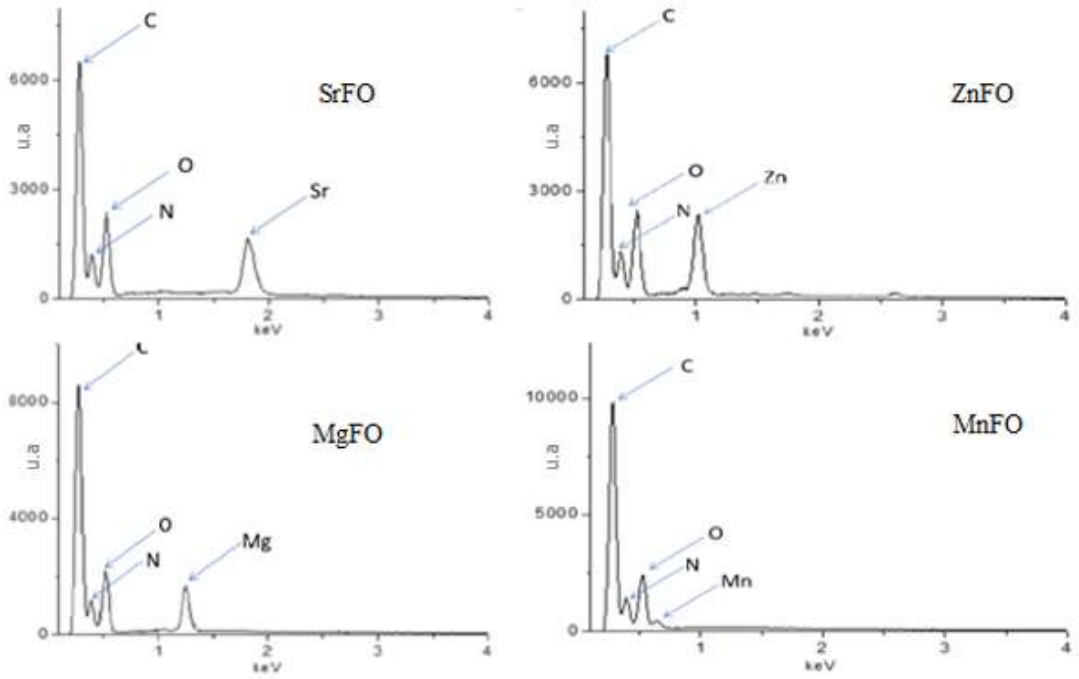

Figure 7- EDS spectra registered for strontium folate (SrFO), zinc folate (ZnFO), magnesium folate (MgFO) and manganese folate (MnFO) complexes.

4.2. ATR-FTIR of Folic Acid Derivatives and Oxidized Polysaccharides

Coordination between the carboxylic group of the folate derivatives and the different cations has been described in the literature indicating the possibility of chelating mode through monodentate or bidentate bridging. The methodology to explain these two modes by taking into consideration the direction of the frequency shift of the υ_{asy} COO- and υ_s COO- vibration bands with respect to those of the free ions has been explained [128]. FTIR spectra of folic acid and folate compounds are showed in Figure 8 and the main vibrational bands are represented in Table 5. The main relevant range is contempled between 1,800 and 1,300 cm^{-1} with the purpose of atributting the coordination modes of the distinct folates. The strong vibration band observed at 1,690 cm^{-1} for folic acid corresponds to the free carboxylic group (COOH), which does not appear in the respective spectra for coordinated compounds (COO-M). Though, there are two bands at 1,604 cm^{-1} and 1,518 cm^{-1} that are related to υ_{asy} COO^- and at 1,412 cm^{-1} corresponding to υ_s COO^- of the folate derivatives. It can be seen that both the υ_{asy} COO^- and υ_s COO^- frequencies moved to lower frequencies to the same extent, which means that the compounds prepared were bridging a bidentate [33,133]

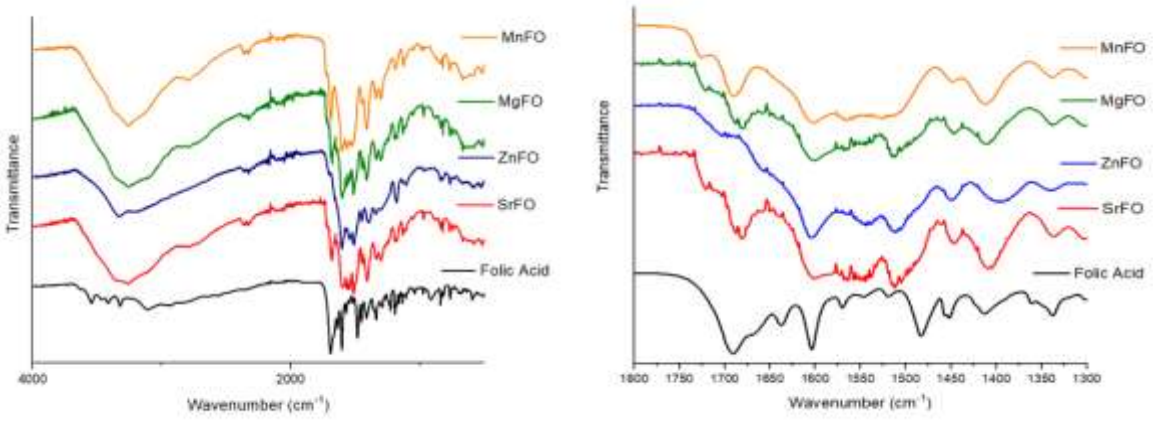

Figure 8- ATR-FTIR spectra obtained for folic acid, strontium folate (SrFO), zinc folate (ZnFO), magnesium folate (MgFO) and manganese folate (MnFO) complexes (left). Region of interest for fingerprint determination (right).

Table 5- ATR-FTIR main frequency assignments (cm-1) of folic acid and folate derivatives.

Assignments	Folic Acid	SrFO	ZnFO	MgFO	MnFO
υ(OH); H_2O	3,545-3,417	3,552	3,575	3,644	3,652
υ(NH)	3,322	3,337	3,322	3,359	3,366
υ_{as} (CH)	3,109	3,124	3,151	3,100	3,195
υ_s(CH)	2,975-2,973	2,903-2,857	2,943-2,911	2,935-2,847	2,870-2,810
υ(COOH)	1,690	-	-	-	-
υ_{as} (COO^-)	1,604-1518	1,511	1,512	1,512	1,525
υ_s(COO^-)	1,412	1,404	1,398	1,411	1,412
υ(CN)	1,182	1,178	1,179	1,178	1,192
δ(CC)	762	767	766	740	767

Chemical modification of oxidized polysaccharides HA-OX and Dex-Ox were analysed by ATR-FTIR. The registered spectra (Figure 9) confirms the diferences between the comercial substances and the modified products. The main difference that matters to be reported is the appearance of broad family of bands from 1,725 – 1,732 cm^{-1} (υ C=O) associated to aldehyde groups that can be observed only in HA-Ox [134, 135] (cm^{-1}) and Dex-Ox [136, 137], respectively.

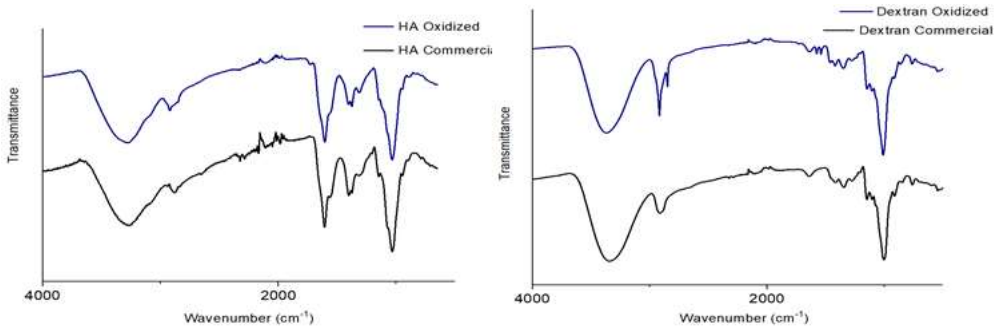

Figure 9- ATR-FTIR spectra obtained for hyaluronic acid (HA), dextran (Dex) and their respective oxidized derivatives HA-Ox and Dex-Ox.

4.3. SEC Cromatography of Oxidized Polysaccharides

The reference technique in the characterization of polymers is the size exclusion chromatography (SEC), which separates the different populations in accordance with the hydrodynamic volume, which can be translated to molecular weight and the polydispersity index. The molecular weight is a key property of polymers, defining certain macroscopic characteristics, such as solubility, viscosity and clearance rates in biological systems [138].

The molecular weight of the reacting polymers is of a great influence regarding the preparation of hydrogels, since they can affect the mobility of reacting molecules or can be responsible for the packing of the reticulated network. For instance, distinct pore size in hydrogels is made by several molecular sizes and molecular weights of polymer probes [139,140].

Dextran is a glucose-based polymer available in several molecular weights and contain a high density of hydroxyl groups that make the polymers highly hydrophilic and capable of being further functionalized chemically [141,142].

HA is biocompatible, biodegradable, nontoxic, non-immunogenic, and has numerous sites for modification with reactive groups [143, 144].

As mentioned before, the aldehyde group is only seen in highly oxidized samples (1730 cm^{-1}). It is reported that the aldehyde groups react with nearby hydroxyl groups, originating hemiacetals or hemialdals [141]. These occurrence could affect the oxidation evolution. The most significant consequence regarding this modification is the final oxidation degree. It determines the dex-Ox gelation rate on hydrogel formulations [141].

Several ways have been used to approach the problem regarding the evaluation of the oxidation degree. Colorimetric titration such as hydroxylamine hydrochloride and the TNBS assay are examples that have been used on mild oxidations [141]. Mild oxidations have the ability to degrade dextran, leading to slight molecular weight decrease. The elimination of the glucose residue, leading to production of aldehydes, could contribute to change the dex-Ox behavior in solution [142].

The molecular weight distributions and M_w/M_n of the four polymers was determined and is represented in Figure 10 and Table 6.

Table 6- Characteristics of native dextran and HA and the oxidized samples. Weight average molecular weight (Mw), Number Average Molecular Weight (Mn) and Polidispersity Index (PDI) calculated by SEC.

Sample	M_w (KDa)	M_n (KDa)	PDI[a]
Dextran	63978	51164	1.25
Dex-Ox	62186	47672	1.30
HA	727426	425978	1.71
HA-Ox	194258	23554	8.25

[a] Polydispersity index corresponding to M_w/M_n

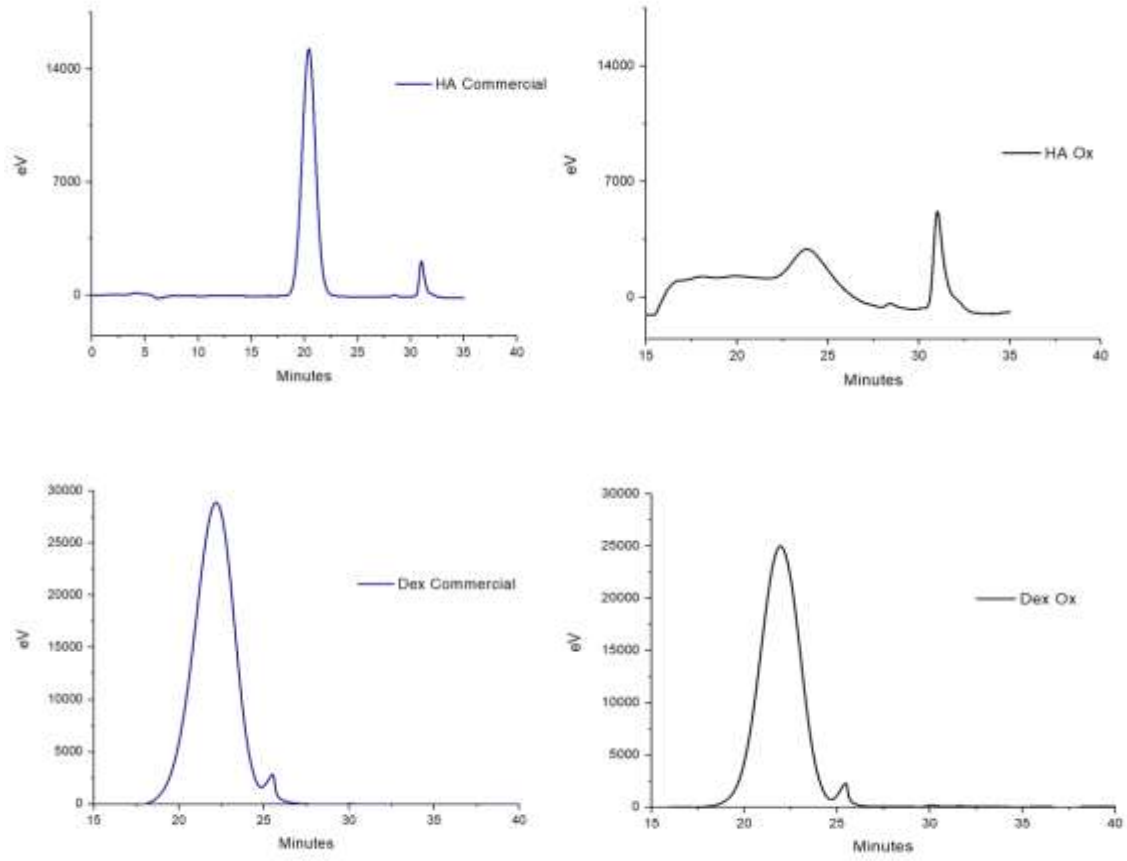

Figure 10- SEC distributions obtained for hyaluronic acid (HA), dextran (Dex) and their respective oxidized derivatives HA-Ox and Dex-Ox.

The molecular weight distribution and the observed differences according to the average molecular weight shows that the molecular weights decrease statistically.

The obtained values of average molecular weights of Dex-Ox samples were of 62 kDa and polydispersity index (M_w/M_n) of 1.30. This values supports the hypothesis that one consequence of the dextran oxidation are the decreased average molecular weight and polydispersity increase [142]. The decreased average molecular weight is related to cleavage of the oligosaccharide during oxidation.

The data also indicate that the reaction modifies the molecular weight of HA. The obtained values of average molecular weights of HA-Ox samples were of 194 kDa and polydispersity index (M_w/M_n) of 8.25. As expected, the degree of oxidation obtained experimentally for HA-Ox derivatives was lower than the theoretical values, and this may be explained by the cleavage of the oligosaccharide (chain scission) [143,144].

These molecular weights allowed the solubilization of the products in aqueous buffered media and flow through injection device in a concentration of 17 % w/v or lower.

4.4. DSC Thermograms of Folic Acid Derivatives

DSC is responsible to measure and analyze the reaction of substances to heat. It determines in a quantitative way the amount of heat absorbed or evolved by a sample as compared to a reference during a specific thermal transition [145]. The modifications experienced by the thermal properties of the samples can be determined isothermally as a function of time or at a constant heating or cooling rate as a function of temperature. Properties such as the heat capacity, the thermal stability and the melting temperature are investigated through the obtained DSC curve [146].

The definition of melting points are very important to determine the chemical structure and purity of correlated substances. On this regard increasing the melting temperature might indicate the transformation of the chemical structure into a more stable one. DSC analysis is very often supported by thermogravimetric analysis.

Regarding the onset of degradation for the five different complexes, it begins to occur after the melting points observed at 220 ºC for folic acid, 350 ºC for SrFO, 320-350 ºC for ZnFO, 350 ºC for MnFO and 360 ºC for MgFO as shown in Figure 11. The melting points are in all cases approximately 100 ºC higher than folic acid which demonstrates greater stability. It proves that the chemical reaction led to the stabilization of the structure.

As can be seen in the Figure, the behavior of ZnFO it is different from the other compounds, so the range of values for the onset of degradation of this complex varies more when compared to the other ones. Despite this difference in the behavior of ZnFO, the melting points for the five different complexes are in agreement with other reported works [103,147,148,149]. The difference observed could be related with lower degree cristalinity between ZnFO and the other compounds.

The DSC curves have proved the thermal stability feature of folate complexes. The results obtained through these analysis show that the behavior of the synthetized metal-folate complexes is in agreement with folic acid thermal stability and with other folate–metal complexes reported by distinct authors. Also, regarding the DSC analysis it demonstrates the formation of proposed compounds [33,126,147,148,149].

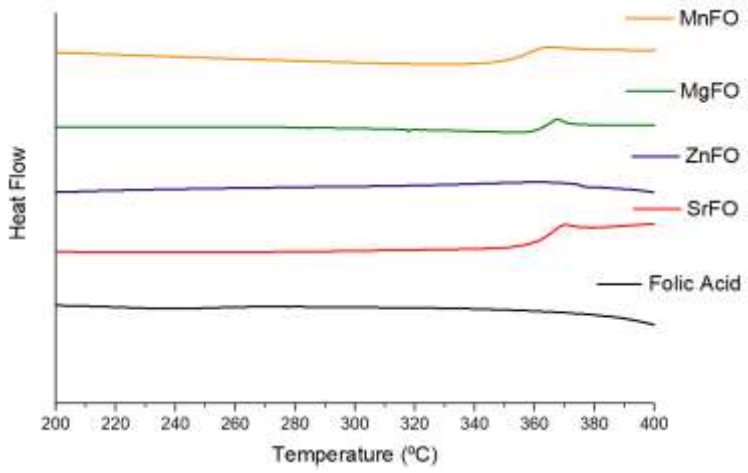

Figure 11- DSC thermograms of folic acid, strontium folate (SrFO), zinc folate (ZnFO), magnesium folate (MgFO) and manganese folate (MnFO) complexes.

4.5. TGA Thermograms of Folic Acid Derivatives

There are few reported works in the literature regarding thermal studies involving folic acid or its metal derivatives [103]. The published work deals with the thermal stability of folic acid or its derivatives in the solid state [132, 150] or the synthesis and characterization of some metal complexes of folic acid [33, 147].

TGA is used to evaluate the thermal stability of a material, in which changes in weight are measured as a function of increasing temperature [151]. It also gives information about the higher use temperature of a material, which means that above that temperature the material will degrade.

Folic acid and the folate derivatives complexes lose weight when submitted to a heating treatment under an inert atmosphere, as can be seen in Figure 12. The first region of weight loss corresponds to the thermodesorption of physically adsorbed water. Also, the folate derivatives that show a decreased value of weight loss in this region indicates an increasing hydrophobic character [152]. So, before the temperature of 175 ºC the first weight loss recorded for SrFO, ZnFO, and MnFO is due to dehydration which matches with the loss of four molecules of water and five molecules of water for MgFO. These values correspond to the proposed molecular formula displayed in Table 7.

The weight loss between 175 and 800 ºC is attributed due to the oxidation of organic matter [103]. So, from 175 ºC on, the degradation profile of the distinct synthetized compounds shows a relevant increase in thermal stability regarding the folic acid salt as reflected on the variation of the onset values associated to the second weight loss step from 194 ºC (folic acid) to 298 ºC (SrFO), 254 ºC (ZnFO), 257 ºC (MgFO) and 246 ºC (MnFO). These results are well correlated with DSC analysis once both showed that the different complexes displayed a relevant increase in thermal stability.

The temperature for a 50 % weight loss from 436 ºC (folic acid) to 690 ºC (SrFO), 650 ºC (ZnFO), 592 ºC (MgFO) and 504 ºC (MnFO).

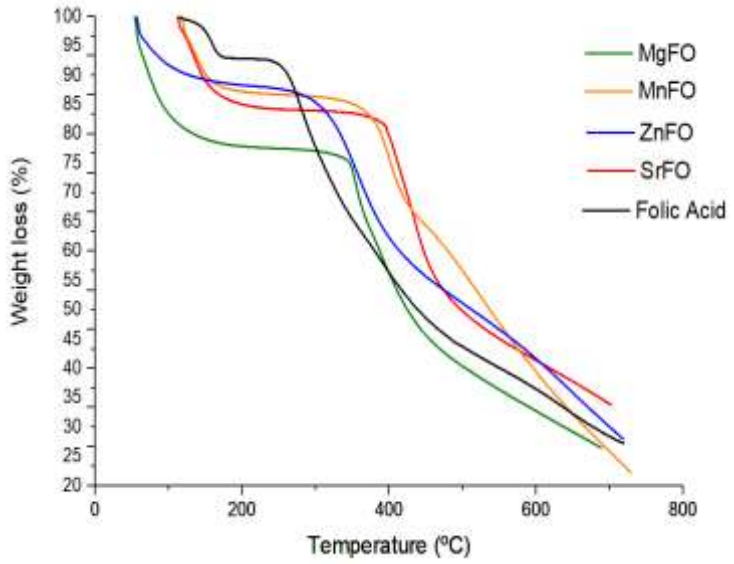

Figure 12- TGA thermograms of folic acid, strontium folate (SrFO), zinc folate (ZnFO), magnesium folate (MgFO) and manganese folate (MnFO) complexes.

4.6. DRX of Folic Acid Derivatives

X-ray diffraction is the ideal non-destructive analytical method for characterizing many types of materials, such as metals, polymers, ceramics, biomaterials, and composites. It has been widely used for material science and engineering, drug discovery and processing control, and many emerging applications [153].

In recent years, the use of two-dimensional diffraction detectors has dramatically increased due to the advances in detector technology. A two-dimensional diffraction pattern contains abundant information about the atomic arrangement and microstructure of materials, as it also observed in melting points [153].

For that reason, DRX analysis provide information regarding the differences of crystallinity and structure between the folic acid and the folate derivatives complexes.

As can be seen in Figure 13, one low-angle peak is identified in SrFO and MgFO at 2.77º, corresponding to a d spacing of 0.34 Å. Two low-angle peaks are identified at the d-spacing of 0.55 Å (2θ =4.51º) for all the samples except for ZnFO and at 1.07 Å (2θ = 8.70). This values are in agreement wtih a 2D hexagonal lattice for all samples. The diferences observed indicate variations in the crystalline structure of the compounds. The reflection peak around 17.86º (d spacing of 2.20 Å) is detected in three different structures (SrFO, ZnFO and MnFO). These similarities between structures correlate well with a repeat distance between the tetramer stacks. Regarding other study, it is expected that the low angle peaks of the samples broaden with higher synthesis temperature. That can indicate a loss of long-range hexagonal packing [154].

The high-angle diffractograms reveal the stacking of folate tetramers, with d spacing of 3.31 Å (2θ =26.93º) for SrFO, 3.32 Å (2θ =27.02º) for ZnFO, 3.35 Å (2θ =27.21º) for MgFO and 3.26 Å (2θ =26.52º) for MnFO.

These values are consistent with previously published data [33, 148, 154] and indicate the formation of a 2D hexagonal lattice. It also demonstrates the passage from a crystalline structure to a more amorphous structure.

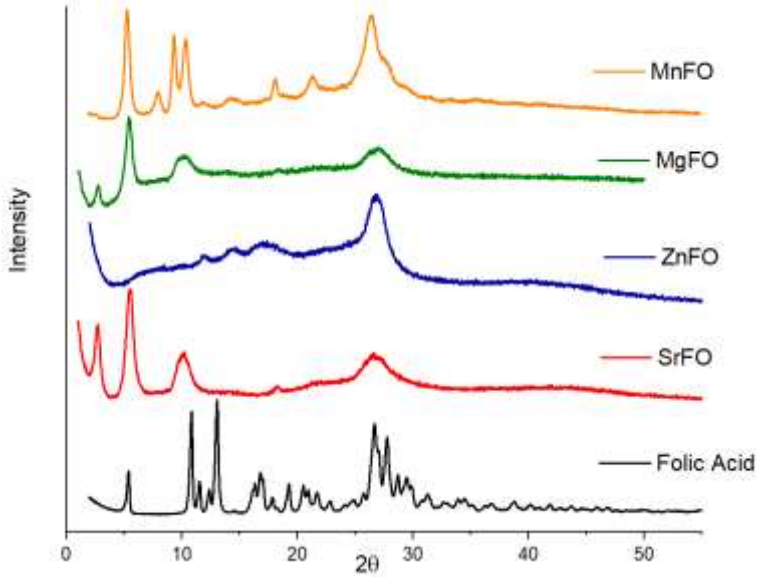

Figure 13- DRX obtained for folic acid, strontium folate (SrFO), zinc folate (ZnFO), magnesium folate (MgFO) and manganese folate (MnFO) complexes.

4.7. Cell Viability of Folate Derivatives

Biological assays for evaluating the biocompatibility of materials can be performed through a wide variety of *in vitro* and *in vivo* tests. Such tests may provide useful information regarding the interaction of the material with the physiological environment and the possible risks associated with its application, thus enabling the identification of materials that are not suitable for use in clinical studies [155]. The type of citotoxicity used was the indirect contact test.

The general toxicity of the folate complexes was evaluated according to the folic acid content on the samples. The more cytotoxic the samples are, the lower the cell viability (%) present will be (Figure 14).

According to the ISO 10993-5 standard [156], a cytotoxic behavior of a material is considered when cell growth decreases below 70 % with respect to that of the reference [155].

Concerning the cytoxicity assays, the analysis that were made revealed that between the four formulations studied, the derivative compounds do not show cytotoxicity except for ZnFO when has a concentration higher than 0.06 mg/mL. The best concentration to work is less than 0.5 μg/mL [33]. It is reported that the derivatives compounds show less toxicity than folic acid free [33].

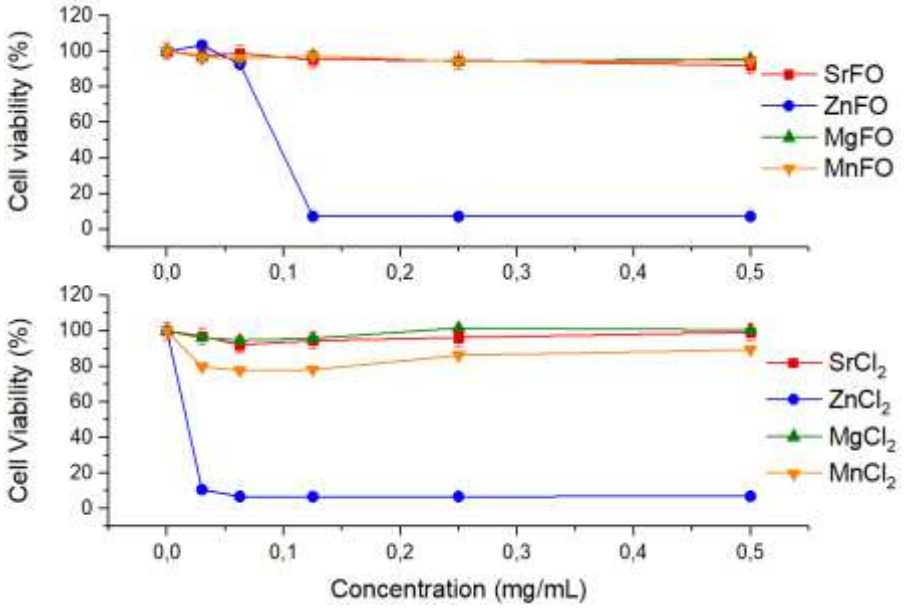

Figure 14- Cytotoxicity assay of hMSC for the metal folate complexes and commercially available metal chloride salts as determined by alamar Blue assay.

For comparison purposes, cytotoxicity of commercial analog metal chlorides was also evaluated and results are displayed as well in Figure 14. Results show that again the Zn salt was the most cytotoxic, reflecting even a higher decrease in cell viability than that corresponding to ZnFO. In addition, a concentration of 0.03 mg/mL is enough to show a considerable cytotoxicity. This result manifests the good biocompatibility of the folate anion.

Zinc has a significant function regarding cell development and growth, immune and nervous system and is an extremely important component of the cell membrane repair machinery and musculoskeletal matrix regeneration. Several enzymes need Zn as a cofactor for their catalytic function [157]. Regarding the bone, Zn has a structural funtion in the bone matrix and is also involved in the preservation of bone mass by stimulating bone formation by osteoblasts and inhibition of bone resorption by osteoclasts [106]. The dietary intake of Zn for adults varies from 8 to 11 mg/day [158]. An excessive amount of Zn^{2+} in the body may have a negative impact in cause vital organs such as the kidney, liver, spleen, brain and heart [157]. Local toxicity produced by Zn may directly affect bone metabolism with prejudicial effects [157].

Taking into account other works, Popp et al. investigated the effect of Zn^{2+} supplemented osteogenic medium on osteoblastic proliferation and differentiation. It was used different concentrations of Zn (0.20, 0.65 and 2.62 mg/L) and no relevant consequences were reported of such amounts on rat bone marrow stromal cells [159]. It is well known that some Zn concentrations can be harmful and cytotoxic to different cell types. Yamamoto et al. reported

that a Zn concentration of 5.89 mg/L inhibits normal osteoblast function [159]. Ito et al. studied zinc-doped b-tricalcium phosphate and reported that the amount of zinc released from the ceramics guided to an important increase regarding the proliferation of osteoblastic MC3T3-E1 cells at 3.53 mg/L in comparison with the ceramics without the presence of zinc [159].

Regarding the results presented, it reveals that if the Zn concentration remains within the recommended limits, this folate complex have the possibility of being effectively applied at the lowest concentration that does not demonstrate toxicity. That application will contribute to the increase of the amount of Zn in the human body, making it able to be used for its various functions, as refered before.

4.8. hMSC Viability and Calcium Deposition *in vitro*

Cell viability assays were carried out in order to determine the effect of two selected folate complexes, SrFO and ZnFO, using hMSC. Also, alizarin red staining was used to determine qualitatively the calcium deposition of the gels. The results of the analyses are presented in Figure 15. Previous studies reported that the cell viability was not negatively affected by the presence of the folate derivatives [32] and even showed a significant increase of cell viability for both SrFO and ZnFO compounds when compared with folic acid cells (control group). The cell viability studies with fluorescent labeled hMSC show a high viability for the studied compounds tested at 4 days, observing a full coverage. AO and PI are used to accurately determine cell viability. Both AO and PI are fluorescent nuclear probes that can detect viable, apoptotic, and necrotic cells. AO can permeate both live cells and will stain all nucleated cells to generate green fluorescence. PI can permeate cells with poor membrane integrity and will stain all dead nucleate cells to generate red fluorescence. Both AO and PI stain late apoptotic cells with orange nuclei [131, 132]. In addition, it is reported that incorporation of strontium ions in bone substitutes constitutes a safe and effective way to stimulate proliferation and differentiation of bone mesenchymal stem cells and osteoblasts [128,160,161,162].

Alizarin red staining is responsible for the detection of calcium compounds in synovial fluids. It is used to determine osteogenic differentiation and is able to form *in vivo* precipitates with free ionic calcium [163]. Preliminary study has shown early calcium deposition of cultures treated with the folid acid derivatives. Regarding this result, it is possible to observe a higher

calcification in the folate compounds than in control group, suggesting that both Sr and Zn ions can induce osteogenic differentiation and can have a role on cell replication and differentiation processes.

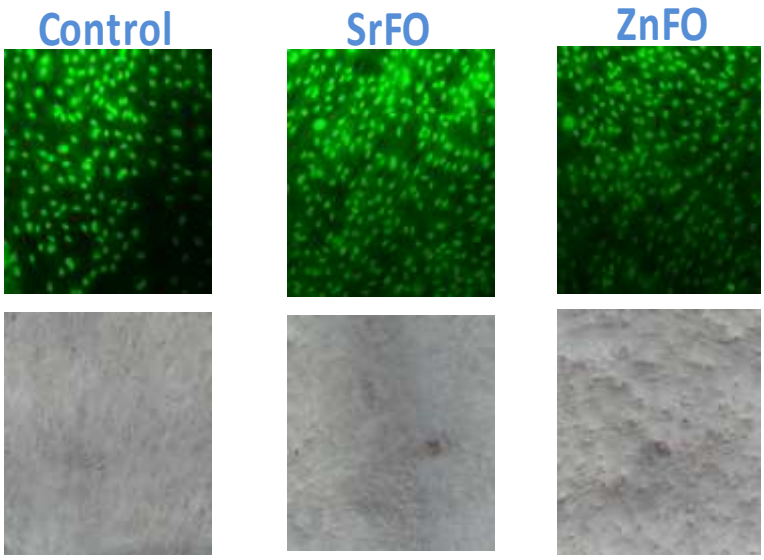

Figure 15- hMSC viability for folate derivatives (upper) and alizarin red staining (lower) showing the calcium deposition for four days (red). MEM culture medium were used as control.

The 2D monolayer cultures have been chosen as in vitro models for cellular research, due to the easy way of set up with little loss of cellular viability. The 2D substrates used in vitro are made from polystyrene or glass, and support cell growth to form a flat, two-dimensional cellular layer [164]. These 2D cultures have a significant role regarding the comprehension of basic cellular biology but they have some limitations such the lack the structural architecture and not all types of epithelial cells can adhere and grow well on the artificial substrates. These facts implicate some limitations regarding the use of standard in vitro techniques [164,165].

In order to improve the relevance of in vitro models, 3D culture models are being increasingly developed. 3D cell culture possess the architectural structure to mimic the in vivo ECM and has the objective of generate cultures which contain the phenotype and functional characteristics of their in vivo counterparts, resulting in a more realistic biological response in vitro. Regarding the cancer research, 3D cultures are beneficial once they mimic events occurring in vivo during progression and formation of cancer [164].

According to Gargotti et al. the study reported that transfer from 2D to 3D culture does not necessarily affect the viability of the cells. When the culture length was increased, the increment in alamar blue conversion were reduced, showing a reduced viability on 3D when compared to a 2D. It was subsequently shown that transfer from 2D to 3D culture can influence cell cycle.

The results of this study highly suggests the use of 3D culture in cytotoxicity assays to improve the relevance of drug, once there is no significant difference in cellular viability [164].

Additional parameters might affect the cell viability and differentiation ability and thus the positive effect of this derivitatives need to be confirmed within the 3D scaffolds.

4.9. Preparation of Folate Derivatives and Hydrogels

MFO derivatives were obtained and purified resulting in yellow-orange fine powders with high yields as can be seen in Table 7. It also displays the theorical values calculated for both metal and coordination water content for each derivative that were obtained by TGA, as explained in Section 4.5. and their good correlation with experimental values confirming the molecular formula proposed.

Table 7- Molecular empiric formula, yield, ICP and elemental analysis, and coordination water of the folate complexes (n=3).

Molecular Formula	Yield[a] (%)	Metal[b] (%At)			Coordination Water[c]		
		Cal		Found	Cal%		Found%
		M.V.	S.D.		M.V.	S.D.	
$SrC_{19}N_7O_{10}H_{25}$($SrFO{\cdot}4H_2O$)	> 95	14.63	0.02	12.22	12.02	0.03	11.90
$ZnC_{19}N_7O_{10}H_{25}$($ZnFO{\cdot}4H_2O$)	> 95	11.71	0.23	11.08	9.67	0.21	9.40
$MgC_{19}N_7O_{11}H_{27}$($MgFO{\cdot}5H_2O$)	> 95	4.39	0.14	4.02	16.76	0	16.76
$MnC_{19}N_7O_{10}H_{25}$($MnFO{\cdot}4H_2O$)	> 95	9.71	0.05	9.07	13.25	0.10	12.72

[a] Determined by gravimetric analysis. [b] Determined by ICP spectroscopy where %At refers to atomic percentage, Cal refers to calculated, M.V. refers to mean value and S.D. refers to standard deviation. [c] Determined by TGA where refers to mean value and S.D. refers to standard deviation

The oxidation of dextran and hyaluronic acid was performed following well described reactions reported in literature [141,166,167]. The use of these derivatives has permitted to prepare biomimetic hydrogels with reduced toxicity in comparison with other methods reported earlier mainly based on the use of glutaraldehyde crosslink [141,166,167].

The oxidation degrees determined by the hydroxilamine titration method are 72 % (n=3 and standard deviation = 0.3) and 78 % (n=3 and standard deviation = 0.4) for and HA-Ox and

Dex-Ox, respectively. It is important to highlight that after the oxidation reaction, the molecular weight distribution and polydispersity of the polysacharides are also affected as discussed in Section 4.3. This fact indicates that the reaction effectively oxidized the 2-3 diol C-C bonds of glucuronic units into dialdehydes but also cause hydrolysis of the polysaccharide backbone, especially for the case of HA. This fact may have also affect to the rheology and reactivity of the HA-Ox containing formulations as it will be discussed in Section 4.10..

The hydrogels were obtained from two different injectable components as indicated in Table 3. The final volume of 1 mL used permitted a good mixture of both components through the mixing needles (Figure 16) and the formation of stable solid materials confirmed by the incerted test tube method in a time range of 8 to 21 min depending of the formulation. This application method may permit the preparation of *in situ* forming hydrogels (Figure 17 and 18) based on biocompatible materials to be used in minimally invasive surgery applications.

Figure 16- Mixing process used to create F1 and F2 formulations.

Figure 17- F1 hydrogels loaded with Sr^{2+} (left) and Zn^{2+} (right).

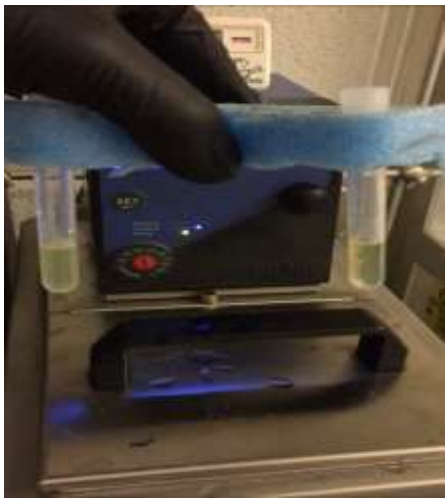

Figure 18- F2 hydrogels loaded with Sr^{2+} (left) and Zn^{2+} (right).

4.10. Rheology

The formation of the two types of hydrogels (F1 and F2) was studied using oscillatory rheometry. This test provides information on the values of the storage modulus (G'), loss modulus (G'') and phase angle (δ) of the hydrogels. At the start of the crosslinking process, the phase angle was about 90°, which is correlated predominantly with a viscous liquid material. As time went on, both G' and G'' increased and the crossover of the two moduli occurred, as expected, at a 45° phase angle. This point is considered as the gel point which is known as the point which passes from being a viscoelastic liquid to a viscoelastic solid [168,169]. Therefore, the time needed to achieve the gel point is used as an indicator of the gelation rate. After the achievement of the gel point, G' continues increasing and G'' reached almost a plateau. At this stage, the phase angle was close to zero, indicating a solid-like elastic material.

In gels loaded with Sr^{2+}, the gel point for each type of hydrogels is different. For dextran-based gels (F1) the time needed to reach the gel point was about 10 min and for HA gels (F2) was about 21 min, as can be seen in Figure 19. This difference may be related with different types of interactions between the hydrogels network of the HA gels and Sr^{2+} or differences in molecular mobility which make the formulation longer to become a gel. The differences regarding the molecular weight and composition of Dex and HA can also explain the distinct time to reach the gel point. Taking into account other studies, a higher concentration of the polysaccharide approached is correlated to a higher viscosity. Thus, a higher viscosity leads to a higher G'. As the concentration

of dex is higher than HA gels, it is expected that the values of G' will be superior on dex gels [170, 171, 172]. This hypothesis will be analyzed deeply in further studies.

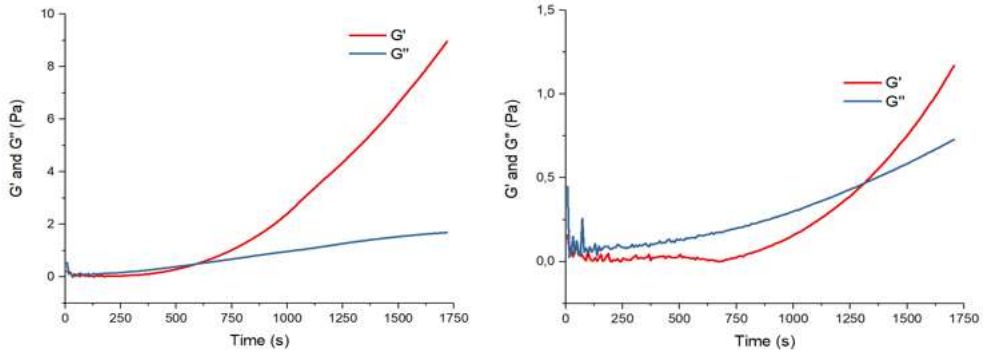

Figure 19- Gelification time for F1 loaded with Sr^{2+} (left) and F2 gels loaded with Sr^{2+} (right).

Regarding gels loaded with Zn^{2+} (Figure 20), the gel points for each type of hydrogels are about 8 min, reaching a viscoelastic solid material. Regarding the differences observed in the values of G' between Figures 19 and 20, these may indicate that the viscosity is dependent on the cation used. For that reason, Zn induces a higher viscosity than Sr. Also, the reason of this difference is out of the scope of this work but will be analyzed in further studies.

These results support the possibility of developing injectable hydrogels formulations based on biomimetic crosslinking agents and bioactive folate derivatives.

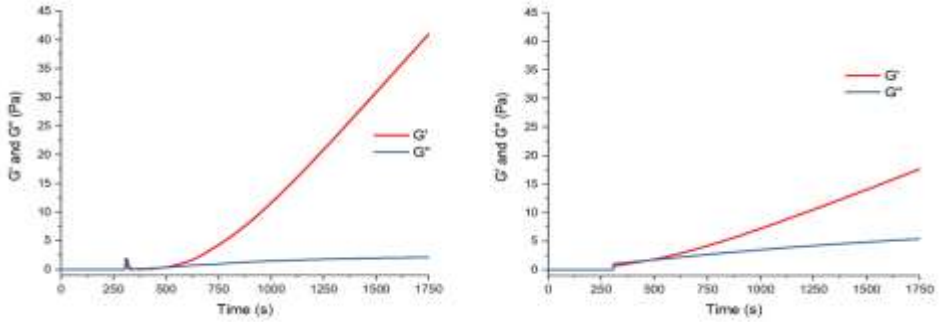

Figure 20- Gelification time for F1 loaded with Zn^{2+} (left) and F2 gels loaded with Zn^{2+} (right).

4.11. Release Profile of Sr^{2+}, Zn^{2+} and Folic Acid

The Sr and Zn released values were obtained by ICP while folic acid was determined by UV-VIS. The amount of each compound released from injectable formulations at different times are shown in Table 8 and 9. The cumulative release profiles are represented in Figures 21 and 22.

Table 8- Mean values (M.V.) and standard deviation (S.D.) of the quantity of Sr and Zn released for each hydrogel formulation (n=3).

Time (h)	Gels							
	Dex+SrFO (mg/L)		Dex+ZnFO (mg/L)		HA+SrFO (mg/L)		HA+ZnFO (mg/L)	
	M.V.	S.D.	M.V.	S.D.	M.V.	S.D.	M.V.	S.D.
2	0.0110	0.0040	0.0020	0	0.0310	0.0096	0.0080	0
4	0.0160	0.0038	0.0023	0	0.0380	0.0095	0.0095	0
24	0.0510	0.0111	0.0050	0.0015	0.0500	0.0192	0.0210	0.0028
96	0.0560	0.0142	0.0140	0.0313	0.0567	0.0042	0.0280	0
168	0.0600	0.0020	0.0190	0.0245	0.0593	0.0015	0.0330	0.0042
336	0.0680	0.0180	0.0240	0.0161	0.0600	0.0079	0.0410	0.0071

Table 9- Mean values (M.V.) and standard deviation (S.D.) of the quantity of Folic Acid released for each hydrogel formulation (n=3).

Time (h)	Gels							
	Dex+SrFO (mg/L)		Dex+ZnFO (mg/L)		HA+SrFO (mg/L)		HA+ZnFO (mg/L)	
	M.V.	S.D.	M.V.	S.D.	M.V.	S.D.	M.V.	S.D.
2	0.0100	0	0.0100	0	0,0230	0.0116	0,0400	0.0071
4	0.0100	0	0.0100	0	0,0400	0.0100	0,0900	0.0141
24	0.0660	0.0635	0.0680	0.0465	0,2370	0.0586	0,1900	0.0141
96	0.1530	0.0379	0.1500	0.0289	0,2500	0.0400	0,2100	0.0707
168	0.2100	0.0361	0.2400	0.0100	0,3900	0.0608	0,3400	0.0778
336	0.3960	0.0513	0.3300	0.0800	0,4670	0.0058	0,5900	0.0071

In order to study the mechanism of the drug release from samples, the release data was fitted to the Higuchi square root of time model, which is normally applied for modeling diffusion-controlled processes of drug release [173-175]. Moreover, the drug release data was fitted to the first order model which represents the release of drug from a system where the release rate is concentration dependent. This model is characterized as log cumulative percent drug remaining versus time.

F1 and F2 based hydrogels show differences in metal ion release kinetics depending on the type of folate and formulation composition (Figures 21 and 22). In the case of F1 (Figure 21), Sr shows a burst release [176] of almost 45 % of the amount delivered in the first 24 h followed by a sustained delivering of the remaining content up to 50 % in 14 days. Conversely, Zinc maintains a constant release rate riseing to a maximum of 30 % in the same time range. This profile can be beneficial for cell surviving as prevalence the concentration of Sr over Zn reaching favorable ion concentrations of 0.009 and 0.090 mg/L and 0.015 and 0.065 mg/L for Sr [33] and Zn [177] respectively, during the period of study. Regarding the release of folic acid, relatively to SrFO the amount delivered and the behavior of the curve is not similar. SrFO shows a slower release of 10 % of the amount delivered in the first 24 h followed by a sustained delivering of the remaining content up to 30 % in the same period, so it is possible to argue that the folic acid is dissociated and released independently of his contraion. On the other hand, ZnFO shows a similar behavior of Zinc, having an identical release rate with a maximum of 30 % as well. For that reason, this demonstrates that folic acid is being released in the form of ZnFO mainly.

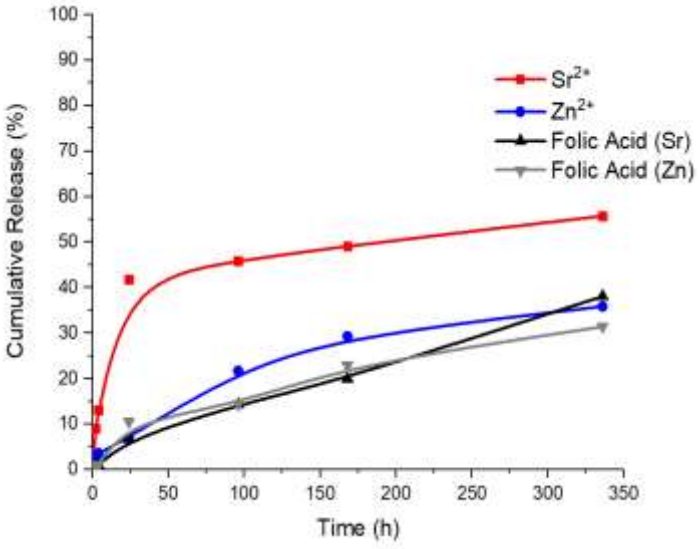

Figure 21- Release curve of strontium, zinc and folic acid obtained from F1 gels in a phosphate buffered reaction medium (37 ºC, pH=7.4)

On the other and, F2 based hydrogel (Figure 22) show a similar Sr release profile reaching a 40 % of cumulative relase in the first 24 hours and delivering up to 45 % during the period of study. Surprisingly, in the case Zn also showed a similar behavior of burst release but in that case with a much higher amount of metal ion released (60 %) after 14 days. Also, this

profile can be beneficial for cell surviving as prevalence the concentration of Sr over Zn reaching favorable ion concentrations of 0.009 and 0.090 mg/L and 0.015 and 0.065 mg/L for Sr [33] and Zn [177] respectively, during the period of study. Regarding the release of folic acid, both SrFO and ZnFO have similarities on the behavior of the curve but slightly differences concerning the amount delivered. SrFO shows a slower release of 4 % of the amount delivered in the first 24 h followed by a sustained delivering of the remaining content up to 40 % 14 days later. In the case of ZnFO also a much higher amount of metal ion released (56 %) during the time of study, suggesting, for F2 hydrogels that folic acid is being released in the form of MFO mainly.

Folic acid is needed to ensure healthy function of numerous processes of the human body including the production of new cells and the role of a co-enzyme in the normal DNA synthesis [103].

The ions in the release medium have an impact in the release of the folic acid by disrupting the folate assembly because they interact with the ions which have cross-linked the folate stacks. Due to the elevated monovalent salt content of PBS, more ions are present in the release medium which causes more disruption of folate assembly [178].

According to Y. Song et al. that prepared a hybrid gel based on folic acid and agar, this kind of non-toxic materials with self-healing property and shear-thinning behavior are broadly applicable regarding the subject of drug release [178]. Regarding the behavior of the release profile of folic acid hydrogels, it can be divided into initial burst release, controlled release and equilibrium release periods. The initial burst release occurs due to a great differential concentration between the medium and gels. Despite the differences between the values of cumulative release between this work and Y. Song et al. both present an analog behavior [178].

Although a study was not made regarding the degradation profile of these gels, it is important to mention that after 14 days, the gels kept the 3D shape confined in the transwell.

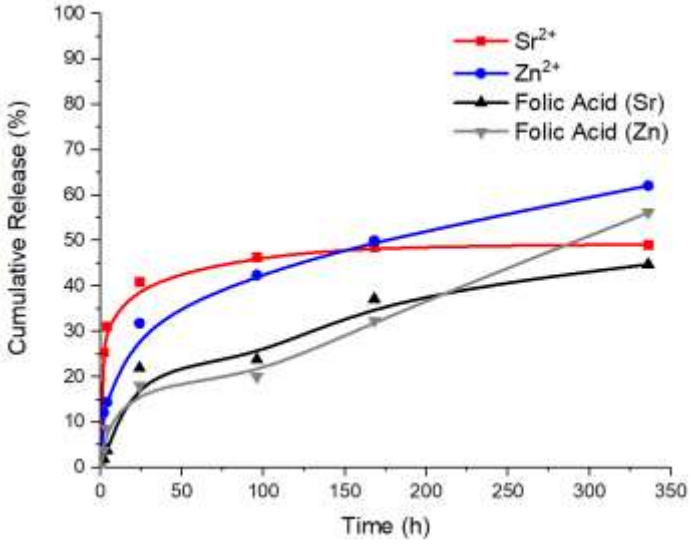

Figure 22- Release curve of strontium, zinc and folic acid obtained from F2 gels in a phosphate buffered reaction medium (37 ºC, pH=7.4)

5. Conclusions

The present work constitutes a novel approach to the preparation of injectable biomimetic formulations made of natural polymers loaded with bioactive folic acid derivatives coordinated with bioactive divalent cations such as Sr, Zn, Mg and Mn for their potential application in musculoskeletal tissue engineering.

The molecular structure of the MFO compounds presents bidentade coordination through COO^- groups. The folate derivatives were non-cytotoxic for hMSC at concentrations lower than 0,06 mg/mL only for one of the formulations and induced calcium deposition to hMSCs cultured *in vitro*.

Also, biomimetic precursors of extracellular matrices were successfully obtained from the oxidation reactions of hyaluronic acid or dextran. These derivatives were capable to react with gelatin in the presence of folate derivatives under physiological conditions forming cross-linked networks in a range of 8-20 minutes.

Truly, these biomimetic injectable formulations based on natural polymers loaded with folic acid derivatives show appropriate features for their application in non-invasive musculoeskeletal tissue engineering applications, with the advantage of avoiding the use of growth factors that usually limited their transition into clinic as consequence of their undesired problems associated with stability and bioaviability of protein-based cell signaling molecules.

6. Future Perspectives

Future work should focus on the effect of the different MFO to promote MSC differentiation and their potential to express specific bone phenotypes trough rtPCR and inmunohistochemical analysis. Regarding the hydrogel formulations, their capacity to laden with living cells need to be tested and perhaps adjust the formulation composition in order to permit high cell viability and injectability. The hydrodynamic properties of injectable formulations and crosslinking time, together with mechanical properties of final formulations need to be accurately determined by additional rheological properties.

In vitro behavior properties of hydrogels must be analized in terms of degradation and swelling capacity.

Depending on the results obtained with human cells and *in vitro* behavior of formulations, further investigations concerning in vivo animal models need to be assessed in order to provide accurate information about safety and potential biological activity towards the translation to clinical applications.

References

[1] Pina, S., Oliveira, J. M., & Reis, R. L. (2015). Natural-based nanocomposites for bone tissue engineering and regenerative medicine: A review. *Advanced Materials*, *27*(7), 1143-1169.

[2] Lavik, E., & Langer, R. (2004). Tissue engineering: current state and perspectives. *Applied microbiology and biotechnology*, *65*(1), 1-8..

[3] Stupp, S. I. (2005). Biomaterials for regenerative medicine. *Mrs Bulletin*, *30*(7), 546-553.

[4] Wang, Y. K., Yong, T., & Ramakrishna, S. (2005). Nanofibres and their influence on cells for tissue regeneration. *Australian journal of chemistry*, *58*(10), 704-712.

[5] EUMUSC. (2013). Musculoskeletal Health in Europe, 12. Retrieved from http://www.eular.org/myUploadData/files/EU_eumusc.net_Report_final.pdf.

[6] Judge, A., Welton, N. J., Sandhu, J., & Ben-Shlomo, Y. (2010). Equity in access to total joint replacement of the hip and knee in England: cross sectional study. *Bmj*, *341*, c4092.

[7] Borkhoff, C. M., Hawker, G. A., & Wright, J. G. (2011). Patient gender affects the referral and recommendation for total joint arthroplasty. *Clinical Orthopaedics and Related Research®*, *469*(7), 1829-1837.

[8] WHO Scientific Group on the Burden of Musculoskeletal Conditions at the Start of the New Millennium. (2003). The burden of musculoskeletal conditions at the start of the new millennium. *World Health Organization technical report series*, *919*, i.

[9] Lingren, L, Gomez-Barrena, E, Duda, G. N, Puhl, W, Carr, A. (2014). European musculoskeletal health and mobility in Horizon 2020: SETTING PRIORITIES FOR MUSCULOSKELETAL RESEARCH AND. *Bone Joint Res*, *3*(3).

[10] Rachner, T., Khosla, S., Hofbauer, L., & Manuscript, A. (2011). New Horizons in Osteoporosis. *Lancet*, *377*(9773), 1276–1287.

[11] Svedbom, A., Hernlund, E., Ivergård, M., Compston, J., Cooper, C., Stenmark, (2013). Osteoporosis in the European Union: A compendium of country-specific reports. *Archives of Osteoporosis*, *8*(1–2).

[12] Ström, O., Borgström, F., Kanis, J. A., Compston, J., Cooper, C., McCloskey, E. V., & Jönsson, B. (2011). Osteoporosis: Burden, health care provision and opportunities in the EU. *Archives of Osteoporosis*, *6*(1–2), 59–155.

[13] Glyn-Jones, S., Palmer, A. J. R., Price, A. J., Vincent, T. L., Weinans, H., & Carr, A. J. (2015). Osteoarthritis. *The Lancet*, *386*(9991), 376-387.

[14] Singh, J. A., Saag, K. G., Bridges, S. L., Akl, E. A., Bannuru, R. R., Sullivan, McAlindon, T. (2016). 2015 American College of Rheumatology Guideline for the Treatment of Rheumatoid Arthritis. *Arthritis & Rheumatology*, *68*(1), 1–26.

[15] Cross, M., Smith, E., Hoy, D., Carmona, L., Wolfe, F., Vos, T., ... & Buchbinder, R. (2014). The global burden of rheumatoid arthritis: estimates from the global burden of disease 2010 study. *Annals of the rheumatic diseases*.

[16] Carbonell, J., Cobo, T., Balsa, A., Descalzo, M. A., Carmona, L., & SERAP Study Group*. (2008). The incidence of rheumatoid arthritis in Spain: results from a nationwide primary care registry. *Rheumatology*, *47*(7), 1088-1092.

[17] Pedersen, J. K., Kjær, N. K., Svendsen, A. J., & Hørslev-Petersen, K. (2009). Incidence of rheumatoid arthritis from 1995 to 2001: impact of ascertainment from multiple sources. *Rheumatology international*, *29*(4), 411-415.

[18] Alharbi, S. A. (2015). A Systematic Overview of Osteogenesis Imperfecta. *Molecular Biology*, *5*(1), 1–9.

[19] Shaker, J. L., Albert, C., Fritz, J., & Harris, G. (2015). Recent developments in osteogenesis imperfecta. *F1000Research*, *4*(F1000 Faculty Rev).

[20] Lindahl, K., Langdahl, B., Ljunggren, Ö., & Kindmark, A. (2014). Treatment of osteogenesis imperfecta in adults. *European Journal of Endocrinology / European Federation of Endocrine Societies*, *171*(2).

[21] Silverman, S., & Christiansen, C. (2012). Individualizing osteoporosis therapy. *Osteoporosis International*, *23*(3), 797–809.

[22] Wells, G. A., Cranney, A., Peterson, J., Boucher, M., Shea, B., Welch, V., ... & Tugwell, P. (2008). Alendronate for the primary and secondary prevention of osteoporotic fractures in postmenopausal women. *The Cochrane Library*.

[23] Wells, G. A., Cranney, A., Peterson, J., Boucher, M., Shea, B., Welch, V., ... & Tugwell, P. (2008). Risedronate for the primary and secondary prevention of osteoporotic fractures in postmenopausal women. *Cochrane Database of Systematic Reviews*, (1).

[24] Hochberg, M. C. (2008). Nonvertebral fracture risk reduction with nitrogen-containing bisphosphonates. *Current osteoporosis reports*, *6*(3), 89-94.

[25] Rennert, G., Pinchev, M., & Rennert, H. S. (2010). Use of bisphosphonates and risk of postmenopausal breast cancer. *Journal of Clinical Oncology*, *28*(22), 3577-3581.

[26] Bonnick, S. L., Harris, S. T., Kendler, D. L., McClung, M. R., & Silverman, S. L. (2010). Management of osteoporosis in postmenopausal women: 2010 position statement of The North

American Menopause Society. *Menopause-the Journal of the North American Menopause Society*, *17*(1), 25-54.

[27] Reginster, J. Y. (2014). Cardiac concerns associated with strontium ranelate. *Expert opinion on drug safety*, *13*(9), 1209-1213.

[28] Ringe, J., Burmester, G. R., & Sittinger, M. (2012). Regenerative medicine in rheumatic disease—progress in tissue engineering. *Nature Reviews Rheumatology*, *8*(8), 493.

[29] Ye, K., Felimban, R., Moulton, S. E., Wallace, G. G., Bella, C. D., Traianedes, K., ... & Myers, D. E. (2013). Bioengineering of articular cartilage: past, present and future. *Regenerative medicine*, *8*(3), 333-349.

[30] Ringe, J., & Sittinger, M. (2014). Regenerative medicine: selecting the right biological scaffold for tissue engineering. *Nature Reviews Rheumatology*, *10*(7), 388.

[31] Gothard, D., Smith, E. L., Kanczler, J. M., Black, C. R., Wells, J. A., Roberts, C. A., ... & Rojo, L. (2015). In vivo assessment of bone regeneration in alginate/bone ECM hydrogels with incorporated skeletal stem cells and single growth factors. *PloS one*, *10*(12), e0145080.

[32] Fabbri, M., Soccio, M., Costa, M., Lotti, N., Gazzano, M., Siracusa, V., ... & Vázquez-Lasa, B. (2016). New fully bio-based PLLA triblock copoly (ester urethane) s as potential candidates for soft tissue engineering. *Polymer Degradation and Stability*, *132*, 169-180.

[33] Rojo, L., Radley-Searle, S., Fernandez-Gutierrez, M., Rodríguez-Lorenzo, L. M., Abradelo, C., Deb, S., & San Román, J. (2015). The synthesis and characterisation of strontium and calcium folates with potential osteogenic activity. *Journal of Materials Chemistry B*, *3*(13), 2708-2713.

[34] Del Campo, M. M., Alvarado-Estrada, K., Rojo, L., Sampedro, J. G., Rosales-Ibáñez, R., & San Román, J. (2015). Effect and application of 3D-Scaffolds in restoration of bone defects. *dental materials*, *31*, e65.

[35] Suárez, P., Rojo, L., González-Gómez, Á., & Román, J. S. (2013). S elf-A ssembling Gradient Copolymers of Vinylimidazol and (A crylic) ibuprofen With Anti-Inflammatory and Zinc Chelating Properties. *Macromolecular bioscience*, *13*(9), 1174-1184.

[36] Velasco, D., Réthoré, G., Newland, B., Parra, J., Elvira, C., Pandit, A., ... & San Román, J. (2012). Low polydispersity (N-ethyl pyrrolidine methacrylamide-co-1-vinylimidazole) linear oligomers for gene therapy applications. *European Journal of Pharmaceutics and Biopharmaceutics*, *82*(3), 465-474.

[37] Ndlovu, M., Bedson, J., Jones, P. W., & Jordan, K. P. (2014). Pain medication management of musculoskeletal conditions at first presentation in primary care: analysis of routinely collected medical record data. *BMC musculoskeletal disorders*, *15*(1), 418.

[38] Laria, A., Lurati, A., Marrazza, M., Mazzocchi, D., Re, K. A., & Scarpellini, M. (2016). The macrophages in rheumatic diseases. Journal of inflammation research, 9, 1.

[39] Utomo, L., Bastiaansen-Jenniskens, Y. M., Verhaar, J. A., & van Osch, G. J. (2016). Cartilage inflammation and degeneration is enhanced by pro-inflammatory (M1) macrophages in vitro, but not inhibited directly by anti-inflammatory (M2) macrophages. *Osteoarthritis and cartilage*, *24*(12), 2162-2170.

[40] Dhandayuthapani, B., Yoshida, Y., Maekawa, T., & Kumar, D. S. (2011). Polymeric scaffolds in tissue engineering application: A review. *International Journal of Polymer Science*, *2011*(ii).

[41] Rana, D., Kumar, T. S. S., & Ramalingam, M. (2014). Cell-Laden Hydrogels for Tissue Engineering. *Journal of Biomaterials and Tissue Engineering*, *4*(7), 507–535.

[42] Kachouie, N. N., Du, Y., Bae, H., Khabiry, M., Ahari, A. F., Zamanian, B., ... & Khademhosseini, A. (2010). Directed assembly of cell-laden hydrogels for engineering functional tissues. *Organogenesis*, *6*(4), 234-244.

[43] Burr, D. B., Bellido, T., & White, K. E. (2014). Bone structure and function. In *Rheumatology: Sixth Edition*. Elsevier Inc..

[44] Deluca, H. F. (2011). Historical overview of vitamin D. *Vitamin D*, *I*, 3–12.

[45] Zhang, S., Wang, X., Li, G., Chong, Y., Zhang, J., Guo, X., … Bi, Z. (2017). Osteoclast regulation of osteoblasts via RANK-RANKL reverse signal transduction in vitro. *Molecular Medicine Reports*, *16*(4), 3994–4000.

[46] Li, X., Liu, Y., Wu, B., Dong, Z., Wang, Y., Lu, J., ... & Wang, Z. (2014). Potential role of the OPG/RANK/RANKL axis in prostate cancer invasion and bone metastasis. *Oncology reports*, *32*(6), 2605-2611.

[47] Cummings, S. R., Martin, J. S., McClung, M. R., Siris, E. S., Eastell, R., Reid, I. R., ... & Kutilek, S. (2009). Denosumab for prevention of fractures in postmenopausal women with osteoporosis. *New England Journal of Medicine*, *361*(8), 756-765.

[48] Ullah, I., Subbarao, R. B., & Rho, G. J. (2015). Human mesenchymal stem cells - current trends and future prospective. *Bioscience Reports*, *35*(2), 1–18.

[49] Daley, W. P., Peters, S. B., & Larsen, M. (2008). Extracellular matrix dynamics in development and regenerative medicine. *Journal of Cell Science*, *121*(3), 255–264.

[50] Hynes, R. O. (2009). Extracellular matrix: not just prety fibrils. *Science*, *326*(5957), 1216–1219.

[51] Lu, P., Takai, K., Weaver, V. M., & Werb, Z. (2011). Extracellular matrix degradation and remodeling in development and disease. *Cold Spring Harb Perspect Biol*, *3*(12), 1–24.

[52] Silver, F. H., DeVore, D., & Siperko, L. M. (2003). Invited Review: Role of mechanophysiology in aging of ECM: effects of changes in mechanochemical transduction. *Journal of Applied Physiology*, *95*(5), 2134–2141.

[53] Hynes, R. O., & Naba, A. (2012). Overview of the matrisome-An inventory of extracellular matrix constituents and functions. *Cold Spring Harbor Perspectives in Biology*, *4*(1), 1–16.

[54] Larrañeta, E., Henry, M., Irwin, N. J., Trotter, J., Perminova, A. A., & Donnelly, R. F. (2018). Synthesis and characterization of hyaluronic acid hydrogels crosslinked using a solvent-free process for potential biomedical applications. *Carbohydrate Polymers*, *181*(October 2017), 1194–1205. https://doi.org/10.1016/j.carbpol.2017.12.015

[55] Nikpour, P., Salimi-Kenari, H., Fahimipour, F., Rabiee, S. M., Imani, M., Dashtimoghadam, E., & Tayebi, L. (2018). Dextran hydrogels incorporated with bioactive glass-ceramic: Nanocomposite scaffolds for bone tissue engineering. *Carbohydrate polymers*, *190*, 281-294.

[56] Liu, Y., & Chan-park, M. B. (2009). Biomaterials Hydrogel based on interpenetrating polymer networks of dextran and gelatin for vascular tissue engineering. *Biomaterials*, *30*(2), 196–207.

[57] Matricardi, P., Di Meo, C., Coviello, T., Hennink, W. E., & Alhaique, F. (2013). Interpen-etrating polymer networks polysaccharide hydrogels for drug delivery and tissue engineering. *Advanced Drug Delivery Reviews*, *65*(9), 1172–1187.

[58] Kanematsu, A., Marui, A., Yamamoto, S., Ozeki, M., Hirano, Y., Yamamoto, M., ... & Tabata, Y. (2004). Type I collagen can function as a reservoir of basic fibroblast growth factor. *Journal of controlled release*, *99*(2), 281-292.

[59] Gelse, K., Pöschl, E., & Aigner, T. (2003). Collagens—structure, function, and biosynthesis. *Advanced drug delivery reviews*, *55*(12), 1531-1546.

[60] Kadler, K. E., Baldock, C., Bella, J., & Boot-Handford, R. P. (2007). Collagen at a glance. *Journal of Cell Science*, *120*(Pt 12), 1955–1958.

[61] Kadler, K. E., Hill, A., & Canty-Laird, E. G. (2008). Collagen fibrillogenesis: fibronectin, integrins, and minor collagens as organizers and nucleators. *Current opinion in cell biology*, *20*(5), 495-501.

[62] Ratanavaraporn, J., Damrongsakkul, S., Sanchavanakit, N., Banaprasert, T., & Kanokpanont, S. (2006). Comparison of Gelatin and Collagen Scaffolds for Fibroblast Cell Culture. *Journal of Metals, Materials and Minerals*, *16*(1), 31–36.

[63] Kang, H. W., Tabata, Y., & Ikada, Y. (1999). Fabrication of porous gelatin scaffolds for tissue engineering. *Biomaterials*, *20*(14), 1339-1344.

[64] Chang, C. H., Liu, H. C., Lin, C. C., Chou, C. H., & Lin, F. H. (2003). Gelatin–chondroitin–hyaluronan tri-copolymer scaffold for cartilage tissue engineering. *Biomaterials*, *24*(26), 4853-4858.

[65] Huang, Y., Onyeri, S., Siewe, M., Moshfeghian, A., & Madihally, S. V. (2005). In vitro characterization of chitosan–gelatin scaffolds for tissue engineering. *Biomaterials*, *26*(36), 7616-7627.

[66] Kuijpers, A. J., Engbers, G. H. M., Feijen, J., De Smedt, S. C., Meyvis, T. K. L., Demeester, J., ... & Dankert, J. (1999). Characterization of the network structure of carbodiimide cross-linked gelatin gels. *Macromolecules*, *32*(10), 3325-3333.

[67] Weaver, F. A., Hood, D. B., Zatina, M., Messina, L., & Badduke, B. (2002). Gelatin–thrombin-based hemostatic sealant for intraoperative bleeding in vascular surgery. *Annals of vascular surgery*, *16*(3), 286-293.

[68] Migliaresi, C., & Motta, A. (2014). *Scaffolds for tissue engineering: Biological design, materials, and fabrication*. Pan Stanford.

[69] Kim, B. S., Park, I. K., Hoshiba, T., Jiang, H. L., Choi, Y. J., Akaike, T., & Cho, C. S. (2011). Design of artificial extracellular matrices for tissue engineering. *Progress in Polymer Science*, *36*(2), 238-268.

[70] Ulery, B. D., Nair, L. S., & Laurencin, C. T. (2011). Biomedical applications of biodegradable polymers. *Journal of polymer science Part B: polymer physics*, *49*(12), 832-864.

[71] Varghese, S., & Elisseeff, J. H. (2006). Hydrogels for musculoskeletal tissue engineering. In *Polymers for regenerative medicine* (pp. 95-144). Springer, Berlin, Heidelberg.

[72] Prabhakaran, M. P., Venugopal, J., Kai, D., & Ramakrishna, S. (2011). Biomimetic material strategies for cardiac tissue engineering. *Materials Science and Engineering: C*, *31*(3), 503-513.

[73] Gentsch, R., & Börner, H. G. (2010). Designing three-dimensional materials at the interface to biology. In *Bioactive surfaces* (pp. 163-192). Springer, Berlin, Heidelberg.

[74] Place, E. S., George, J. H., Williams, C. K., & Stevens, M. M. (2009). Synthetic polymer scaffolds for tissue engineering. *Chemical Society Reviews*, *38*(4), 1139-1151.

[75] Bacakova, L., Filova, E., Parizek, M., Ruml, T., & Svorcik, V. (2011). Modulation of cell adhesion, proliferation and differentiation on materials designed for body implants. *Biotechnology advances*, *29*(6), 739-767.

[76] Tan, H., & Marra, K. G. (2010). Injectable, biodegradable hydrogels for tissue engineering applications. *Materials*, *3*(3), 1746-1767.

[77] Tian, H., Tang, Z., Zhuang, X., Chen, X., & Jing, X. (2012). Biodegradable synthetic polymers: preparation, functionalization and biomedical application. *Progress in Polymer Science*, *37*(2), 237-280.

[78] Sato, T., Aoyagi, T., Ebara, M., & Auzély-Velty, R. (2017). Catechol-modified hyaluronic acid: in situ-forming hydrogels by auto-oxidation of catechol or photo-oxidation using visible light. *Polymer Bulletin*, *74*(10), 4069–4085.

[79] Liu, M., Zeng, X., Ma, C., Yi, H., Ali, Z., Mou, X., ... & He, N. (2017). Injectable hydrogels for cartilage and bone tissue engineering. *Bone research*, *5*, 17014.

[80] Slaughter, B. V., Khurshid, S. S., Fisher, O. Z., Khademhosseini, A., & Peppas, N. A. (2009). Hydrogels in regenerative medicine. *Advanced materials*, *21*(32-33), 3307-3329.

[81] Choi, B., Kim, S., Lin, B., Wu, B. M., & Lee, M. (2014). Cartilaginous extracellular matrix-modified chitosan hydrogels for cartilage tissue engineering. *ACS applied materials & interfaces*, *6*(22), 20110-20121.

[82] Van Vlierberghe, S., Dubruel, P., & Schacht, E. (2011). Biopolymer-based hydrogels as scaffolds for tissue engineering applications: a review. *Biomacromolecules*, *12*(5), 1387-1408.

[83] Yazdimamaghani, M., Vashaee, D., Assefa, S., Walker, K. J., Madihally, S. V., Köhler, G. A., & Tayebi, L. (2014). Hybrid macroporous gelatin/bioactive-glass/nanosilver scaffolds with

controlled degradation behavior and antimicrobial activity for bone tissue engineering. *Journal of biomedical nanotechnology*, *10*(6), 911-931.

[84] Kim, D. Y., Kwon, D. Y., Kwon, J. S., Kim, J. H., Min, B. H., & Kim, M. S. (2015). Stimuli-responsive injectable in situ-forming hydrogels for regenerative medicines. *Polymer Reviews*, *55*(3), 407-452.

[85] Puertas-Bartolomé, M., Benito-Garzón, L., & Olmeda-Lozano, M. (2018). In Situ Cross-Linkable Polymer Systems and Composites for Osteochondral Regeneration. Osteochondral Tissue Engineering: Nanotechnology, Scaffolding-Related Developments and Translation, 327-355.

[86] Patenaude, M., Smeets, N. M., & Hoare, T. (2014). Designing Injectable, Covalently Cross-Linked Hydrogels for Biomedical Applications. *Macromolecular rapid communications*, *35*(6), 598-617.

[87] Yang, J. A., Yeom, J., Hwang, B. W., Hoffman, A. S., & Hahn, S. K. (2014). In situ-forming injectable hydrogels for regenerative medicine. *Progress in Polymer Science*, *39*(12), 1973-1986.

[88] Gibbs, D. M., Black, C. R., Dawson, J. I., & Oreffo, R. O. (2016). A review of hydrogel use in fracture healing and bone regeneration. *Journal of tissue engineering and regenerative medicine*, *10*(3), 187-198.

[89] Marques, C. F., Olhero, S. M., Torres, P. M., Abrantes, J. C., Fateixa, S., Nogueira, H. I., ... & Ferreira, J. M. (2019). Novel sintering-free scaffolds obtained by additive manufacturing for concurrent bone regeneration and drug delivery: Proof of concept. *Materials Science and Engineering: C*, *94*, 426-436.

[90] Mora-Boza, A., Puertas-Bartolomé, M., Vázquez-Lasa, B., San Román, J., Pérez-Caballer, A., & Olmeda-Lozano, M. (2017). Contribution of bioactive hyaluronic acid and gelatin to regenerative medicine. Methodologies of gels preparation and advanced applications.

[91] Hoare, T. R., & Kohane, D. S. (2008). Hydrogels in drug delivery: Progress and challenges. *Polymer*, *49*(8), 1993-2007.

[92] Lam, J., Lu, S., Kasper, F. K., & Mikos, A. G. (2015). Strategies for controlled delivery of biologics for cartilage repair. *Advanced Drug Delivery Reviews*, *84*, 123–134.

[93] Lee, K., Silva, E. A., & Mooney, D. J. (2011). Growth factor delivery-based tissue engineering: general approaches and a review of recent developments. *Journal of the Royal Society Interface*, *8*(55), 153-170.

[94] Fortier, L. A., Barker, J. U., Strauss, E. J., McCarrel, T. M., & Cole, B. J. (2011). The role of growth factors in cartilage repair. *Clinical Orthopaedics and Related Research®*, *469*(10), 2706-2715.

[95] Santo, V. E., Gomes, M. E., Mano, J. F., & Reis, R. L. (2013). Controlled release strategies for bone, cartilage, and osteochondral engineering—part I: recapitulation of native tissue healing and variables for the design of delivery systems. *Tissue Engineering Part B: Reviews*, *19*(4), 308-326.

[96] Schmidt, M. B., Chen, E. H., & Lynch, S. E. (2006). A review of the effects of insulin-like growth factor and platelet derived growth factor on in vivo cartilage healing and repair. *Osteoarthritis and cartilage*, *14*(5), 403-412.

[97] Cals, F. L. J., Hellingman, C. A., Koevoet, W., de Jong, R. B., & van Osch, G. J. V. M. (2012). Effects of transforming growth factor-β subtypes on in vitro cartilage production and mineralization of human bone marrow stromal-derived mesenchymal stem cells. *Journal of tissue engineering and regenerative medicine*, *6*(1), 68-76.

[98] Bos, P. K., Van Osch, G. J. V. M., Frenz, D. A., Verhaar, J. A. N., & Verwoerd-Verhoef, H. L. (2001). Growth factor expression in cartilage wound healing: temporal and spatial immunolocalization in a rabbit auricular cartilage wound model. *Osteoarthritis and cartilage*, *9*(4), 382-389.

[99] Fan, H., Tao, H., Wu, Y., Hu, Y., Yan, Y., & Luo, Z. (2010). TGF-β3 immobilized PLGA-gelatin/chondroitin sulfate/hyaluronic acid hybrid scaffold for cartilage regeneration. *Journal of biomedical materials research Part A*, *95*(4), 982-992.

[100] Wang, W., Li, B., Yang, J., Xin, L., Li, Y., Yin, H., ... & Gao, C. (2010). The restoration of full-thickness cartilage defects with BMSCs and TGF-beta 1 loaded PLGA/fibrin gel constructs. *Biomaterials*, *31*(34), 8964-8973.

[101] Guo, X., Park, H., Young, S., Kretlow, J. D., Van den Beucken, J. J., Baggett, L. S., ... & Jansen, J. A. (2010). Repair of osteochondral defects with biodegradable hydrogel composites encapsulating marrow mesenchymal stem cells in a rabbit model. *Acta biomaterialia*, *6*(1), 39-47.

[102] Patil, A. S., Sable, R. B., & Kothari, R. M. (2011). An update on transforming growth factor-β (TGF-β): Sources, types, functions and clinical applicability for cartilage/bone healing. *Journal of cellular physiology*, *226*(12), 3094-3103.

[103] Dametto, P. R., Ambrozini, B., Caires, F. J., Franzini, V. P., & Ionashiro, M. (2014). Synthesis, characterization and thermal behaviour of solid-state compounds of folates with some bivalent transition metals ions. *Journal of Thermal Analysis and Calorimetry*, *115*(1), 161–166.

[104] Akal, Z. Ü., Alpsoy, L., & Baykal, A. (2016). Biomedical applications of SPION@ APTES@ PEG-folic acid@ carboxylated quercetin nanodrug on various cancer cells. *Applied Surface Science*, *378*, 572-581

[105] Cai, C., Lin, P., Zhu, H., Ko, J. K., Hwang, M., Tan, T., ... & Ma, J. (2015). Zinc Binding to MG53 Facilitates Repair of Injury to Cell Membrane. *Journal of Biological Chemistry*, jbc-M114.

[106] Lowe, N. M., Fraser, W. D., & Jackson, M. J. (2002). Is there a potential therapeutic value of copper and zinc for osteoporosis?. *Proceedings of the Nutrition Society*, *61*(2), 181-185.

[107] Mayer, J. (1964). Zinc Deficiency: A Cause of Growth Retardation?. *Postgraduate medicine*, *35*(2), 206-209.

[108] Fukada, T., Yamasaki, S., Nishida, K., Murakami, M., & Hirano, T. (2011). Zinc homeostasis and signaling in health and diseases. *JBIC Journal of Biological Inorganic Chemistry*, *16*(7), 1123-1134.

[109] Flannery, C. R., Little, C. B., Hughes, C. E., & Caterson, B. (2000). Expression of matrix metalloproteinases (MMPs) and disintegrin metalloproteinases (ADAMs) in experimental systems of cartilage matrix degradation. *International Journal of Experimental Pathology*, *81*(1), A12.

[110] Demoor, M., Ollitrault, D., Gomez-Leduc, T., Bouyoucef, M., Hervieu, M., Fabre, H., ... & Legendre, F. (2014). Cartilage tissue engineering: molecular control of chondrocyte differentiation for proper cartilage matrix reconstruction. *Biochimica et Biophysica Acta (BBA)-General Subjects*, *1840*(8), 2414-2440.

[111] Troeberg, L., & Nagase, H. (2012). Proteases involved in cartilage matrix degradation in osteoarthritis. *Biochimica et Biophysica Acta (BBA)-Proteins and Proteomics*, *1824*(1), 133-145.

[112] Rosenberg, K., Olsson, H., Mörgelin, M., & Heinegård, D. (1998). Cartilage oligomeric matrix protein shows high affinity zinc-dependent interaction with triple helical collagen. *Journal of Biological Chemistry*, *273*(32), 20397-20403.

[113] Castiglioni, S., Cazzaniga, A., Albisetti, W., & Maier, J. A. (2013). Magnesium and osteoporosis: current state of knowledge and future research directions. *Nutrients*, *5*(8), 3022-3033.

[114] Li, F. Y., Chaigne-Delalande, B., Kanellopoulou, C., Davis, J. C., Matthews, H. F., Douek, D. C., ... & Lenardo, M. J. (2011). Second messenger role for Mg 2+ revealed by human T-cell immunodeficiency. *Nature*, *475*(7357), 471.

[115] Rude, R. K., Singer, F. R., & Gruber, H. E. (2009). Skeletal and hormonal effects of magnesium deficiency. *Journal of the American College of Nutrition*, *28*(2), 131-141.

[116] Rude, R. K., Kirchen, M. E., Gruber, H. E., Meyer, M. H., Luck, J. S., & Crawford, D. L. (1999). Magnesium deficiency-induced osteoporosis in the rat: uncoupling of bone formation and bone resorption. *Magnesium research*, *12*(4), 257-267.

[117] Rude, R. K., Gruber, H. E., Wei, L. Y., Frausto, A., & Mills, B. G. (2003). Magnesium deficiency: effect on bone and mineral metabolism in the mouse. *Calcified tissue international*, *72*(1), 32-41.

[118] Miola, M., Brovarone, C. V., Maina, G., Rossi, F., Bergandi, L., Ghigo, D., ... & Vernè, E. (2014). In vitro study of manganese-doped bioactive glasses for bone regeneration. *Materials Science and Engineering: C*, *38*, 107-118.

[119] Muszyńska, A., Wołczyński, S., & Palka, J. (2001). The mechanism for anthracycline-induced inhibition of collagen biosynthesis. *European journal of pharmacology*, *411*(1-2), 17-25.

[120] Surazynski, A., Miltyk, W., Palka, J., & Phang, J. M. (2008). Prolidase-dependent regulation of collagen biosynthesis. *Amino acids*, *35*(4), 731-738.

[121] Humphries, M. J. (2000). Integrin structure.

[122] Slørdahl, T. S., Hov, H., Holt, R. U., Baykov, V., Syversen, T., Sundan, A., ... & Børset, M. (2008). Mn2+ regulates myeloma cell adhesion differently than the proadhesive cytokines HGF, IGF-1, and SDF-1α. *European journal of haematology*, *81*(6), 437-447.

[123] Smith, J. W., Piotrowicz, R. S., & Mathis, D. (1994). A mechanism for divalent cation regulation of beta 3-integrins. *Journal of Biological Chemistry*, *269*(2), 960-967.

[124] Helfrich, M. H., Nesbitt, S. A., Lakkakorpi, P. T., Barnes, M. J., Bodary, S. C., Shankar, G., ... & Horton, M. A. (1996). β1 integrins and osteoclast function: involvement in collagen recognition and bone resorption. *Bone*, *19*(4), 317-328.

[125] Bae, Y. J., & Kim, M. H. (2008). Manganese supplementation improves mineral density of the spine and femur and serum osteocalcin in rats. *Biological trace element research*, *124*(1), 28-34.

[126] Hazell, A. S., Desjardins, P., & Butterworth, R. F. (1999). Increased expression of glyceraldehyde-3-phosphate dehydrogenase in cultured astrocytes following exposure to manganese. *Neurochemistry International*, *35*(1), 11-17.

[127] Sriranganathan, D., Kanwal, N., Hing, K. A., & Hill, R. G. (2016). Strontium substituted bioactive glasses for tissue engineered scaffolds: the importance of octacalcium phosphate. *Journal of Materials Science: Materials in Medicine*, *27*(2), 1–10.

[128] Martin-del-Campo, M., Rosales-Ibañez, R., Alvarado, K., Sampedro, J. G., Garcia-Sepulveda, C. A., Deb, S., … Rojo, L. (2016). Strontium folate loaded biohybrid scaffolds seeded with dental pulp stem cells induce in vivo bone regeneration in critical sized defects. *Biomater. Sci.*, *4*(11), 1596–1604.

[129] Marie, P. J., Ammann, P., Boivin, G., & Rey, C. (2001). Mechanisms of action and therapeutic potential of strontium in bone. *Calcified tissue international*, *69*(3), 121-129.

[130] Bryant, W. M. D., & Smith, D. M. (1935). Improved Hydroxylamine Method for the Determination of Aldehydes and Ketones. Displacement of Oxime Equilibria by Means of Pyridine. *Journal of the American Chemical Society*, *57*(1), 57-61.

[131] Salucci, S., Burattini, S., Giordano, F. M., Lucarini, S., Diamantini, G., & Falcieri, E. (2017). Further highlighting on the prevention of oxidative damage by polyphenol-rich wine extracts. *Journal of medicinal food*, *20*(4), 410-419.

[132] Salucci, S., Burattini, S., Battistelli, M., Buontempo, F., Canonico, B., Martelli, A. M., ... & Falcieri, E. (2015). Tyrosol prevents apoptosis in irradiated keratinocytes. *Journal of dermatological science*, *80*(1), 61-68.

[133] Nakamoto, K., & McCarthy, P. J. (1968). *Spectroscopy and structure of metal chelate compounds*. Wiley.

[134] Su, W. Y., Chen, Y. C., & Lin, F. H. (2010). Injectable oxidized hyaluronic acid/adipic acid dihydrazide hydrogel for nucleus pulposus regeneration. *Acta biomaterialia*, *6*(8), 3044-3055.

[135] Weis, M., Shan, J., Kuhlmann, M., Jungst, T., Tessmar, J., & Groll, J. (2018). Evaluation of Hydrogels Based on Oxidized Hyaluronic Acid for Bioprinting. *Gels*, *4*(4), 82.

[136] Li, L., Ge, J., Ma, P. X., & Guo, B. (2015). Injectable conducting interpenetrating polymer network hydrogels from gelatin-graft-polyaniline and oxidized dextran with enhanced mechanical properties. *RSC Advances*, *5*(112), 92490-92498.

[137] Ferreira, M. P., Talman, V., Torrieri, G., Liu, D., Marques, G., Moslova, K., ... & Santos, H. A. (2018). Dual-Drug Delivery Using Dextran-Functionalized Nanoparticles Targeting Cardiac Fibroblasts for Cellular Reprogramming. *Advanced Functional Materials*, *28*(15), 1705134.

[138] Hunt, B. J., & James, M. I. (Eds.). (2012). Polymer characterisation. Springer Science & Business Media.

[139] Ranjha, N. M., & Khan, S. (2013). Chitosan/poly (vinyl alcohol) based hydrogels for biomedical applications: a review. *J. Pharm. Altern. Med*, *2*(1), 30-41.

[140] Khan, S., Ullah, A., Ullah, K., Rehman, N., Khan, S., Ullah, A., … Rehman, N. (2016). *Insight into hydrogels Insight into hydrogels. Designed Monomers and Polymers,* 5551, 0. https://doi.org/10.1080/15685551.2016.1169380

[141] Maia, J., Carvalho, R. A., Coelho, J. F., Simões, P. N., & Gil, M. H. (2011). Insight on the periodate oxidation of dextran and its structural vicissitudes. *Polymer*, *52*(2), 258-265.

[142] Maia, J., Ferreira, L., Carvalho, R., Ramos, M. A., & Gil, M. H. (2005). Synthesis and characterization of new injectable and degradable dextran-based hydrogels. *Polymer*, *46*(23), 9604-9614.

[143] Dosio, F., Arpicco, S., Stella, B., & Fattal, E. (2016). Hyaluronic acid for anticancer drug and nucleic acid delivery. *Advanced drug delivery reviews*, *97*, 204-236.

[144] Highley, C. B., Prestwich, G. D., & Burdick, J. A. (2016). Recent advances in hyaluronic acid hydrogels for biomedical applications. *Current opinion in biotechnology*, *40*, 35-40.

[145] Müller, A. J., & Michell, R. M. (2016). Differential scanning calorimetry of polymers. *Polym. Morphol. Princ. Charact. Process*, 72-99.

[146] Drzeżdżon, J., Jacewicz, D., Sielicka, A., & Chmurzyński, L. (2018). Characterization of polymers based on differential scanning calorimetry based techniques. *TrAC Trends in Analytical Chemistry*.

[147] El-Wahed, M. A., Refat, M. S., & El-Megharbel, S. M. (2008). Synthesis, spectroscopic and thermal characterization of some transition metal complexes of folic acid. *Spectrochimica Acta Part A: Molecular and Biomolecular Spectroscopy*, *70*(4), 916-922.

[148] Vora, A., Riga, A., Dollimore, D., & Alexander, K. (2004). Thermal stability of folic acid in the solid-state. Journal of thermal analysis and calorimetry, 75(3), 709-717.

[149] Hamed, E., Attia, M. S., & Bassiouny, K. (2009). Synthesis, spectroscopic and thermal characterization of copper (II) and iron (III) complexes of folic acid and their absorption efficiency in the blood. Bioinorganic chemistry and applications, 2009.

[150] Dametto, P. R., Caires, F. J., Ambrozini, B., & Ionashiro, M. (2010). Synthesis, characterization and thermal behaviour of light trivalent lanthanides folates on solid state. *Journal of thermal analysis and calorimetry*, *105*(3), 831-836.

[151] Boparai, K. S., Singh, R., Fabbrocino, F., & Fraternali, F. (2016). Thermal characterization of recycled polymer for additive manufacturing applications. *Composites Part B: Engineering*, *106*, 42-47.

[152] de Oliveira Freitas, L. B., Bravo, I. J. G., de Almeida Macedo, W. A., & de Sousa, E. M. B. (2016). Mesoporous silica materials functionalized with folic acid: preparation, characterization and release profile study with methotrexate. *Journal of Sol-Gel Science and Technology*, *77*(1), 186-204.

[153] He, B. B. (2018). *Two-dimensional X-ray diffraction*. John Wiley & Sons.

[154] Atluri, R., Iqbal, M. N., Bacsik, Z., Hedin, N., Villaescusa, L. A., & Garcia-Bennett, A. E. (2013). Self-assembly mechanism of folate-templated mesoporous silica. Langmuir, 29(38), 12003-12012.

[155] Sastre, R., de Aza, S., & San Román, J. (2004). *Biomateriales*. Faenza editrice iberica.

[156] International Standard Organization (ISO) (2009). ISO 10993-5 Biological Evaluation of Medical Devices-Part 5: Tests for In Vitro Cytotoxicity.

[157] Murni, N. S., Dambatta, M. S., Yeap, S. K., Froemming, G. R. A., & Hermawan, H. (2015). Cytotoxicity evaluation of biodegradable Zn–3Mg alloy toward normal human osteoblast cells. Materials Science and Engineering: C, 49, 560-566.

[158] Price, C. T., Langford, J. R., & Liporace, F. A. (2012). Essential nutrients for bone health and a review of their availability in the average North American diet. The open orthopaedics journal, 6, 143.

[159] Haimi, S., Gorianc, G., Moimas, L., Lindroos, B., Huhtala, H., Räty, S., ... & Suuronen, R. (2009). Characterization of zinc-releasing three-dimensional bioactive glass scaffolds and their effect on human adipose stem cell proliferation and osteogenic differentiation. Acta Biomaterialia, 5(8), 3122-3131.

[160] Zhang, J., Zhao, S., Zhu, Y., Huang, Y., Zhu, M., Tao, C., & Zhang, C. (2014). Three-dimensional printing of strontium-containing mesoporous bioactive glass scaffolds for bone regeneration. *Acta biomaterialia*, *10*(5), 2269-2281.

[161] Liao, W., Zhong, J., Yu, J., Xie, J., Liu, Y., Du, L., ... & Han, Z. (2009). Therapeutic benefit of human umbilical cord derived mesenchymal stromal cells in intracerebral hemorrhage rat: implications of anti-inflammation and angiogenesis. *Cellular Physiology and Biochemistry*, *24*(3-4), 307-316.

[162] Caverzasio, J. (2008). Strontium ranelate promotes osteoblastic cell replication through at least two different mechanisms. *Bone*, *42*(6), 1131-1136.

[163] Bensimon-Brito, A., Cardeira, J., Dionísio, G., Huysseune, A., Cancela, M. L., & Witten, P. E. (2016). Revisiting in vivo staining with alizarin red S-a valuable approach to analyse zebrafish skeletal mineralization during development and regeneration. BMC developmental biology, 16(1), 2.

[164] Gargotti, M., Lopez-Gonzalez, U., Byrne, H. J., & Casey, A. (2018). Comparative studies of cellular viability levels on 2D and 3D in vitro culture matrices. Cytotechnology, 70(1), 261-273.

[165] Bonnier, F., Keating, M. E., Wrobel, T. P., Majzner, K., Baranska, M., Garcia-Munoz, A., ... & Byrne, H. J. (2015). Cell viability assessment using the Alamar blue assay: a comparison of 2D and 3D cell culture models. Toxicology in vitro, 29(1), 124-131.

[166] Chen, Y. C., Su, W. Y., Yang, S. H., Gefen, A., & Lin, F. H. (2013). In situ forming hydrogels composed of oxidized high molecular weight hyaluronic acid and gelatin for nucleus pulposus regeneration. *Acta biomaterialia*, *9*(2), 5181-5193.

[167] Weng, L., Romanov, A., Rooney, J., & Chen, W. (2008). Non-cytotoxic, in situ gelable hydrogels composed of N-carboxyethyl chitosan and oxidized dextran. *Biomaterials*, *29*(29), 3905-3913.

[168] Winter, H. H., & Chambon, F. (1986). Analysis of linear viscoelasticity of a crosslinking polymer at the gel point. *Journal of rheology*, *30*(2), 367-382.

[169] Lee, F., Chung, J. E., & Kurisawa, M. (2008). An injectable enzymatically crosslinked hyaluronic acid–tyramine hydrogel system with independent tuning of mechanical strength and gelation rate. *Soft Matter*, *4*(4), 880-887.

[170] Pescosolido, L., Schuurman, W., Malda, J., Matricardi, P., Alhaique, F., Coviello, T., ... & Vermonden, T. (2011). Hyaluronic acid and dextran-based semi-IPN hydrogels as biomaterials for bioprinting. *Biomacromolecules*, *12*(5), 1831-1838.

[171] Anderson, D. (2013). CHARACTERIZATION OF RHEOLOGICAL AND MASS TRANSPORT PROPERTIES OF HYALURONIC ACID FOR MEDICAL USE.

[172] Weng, L., Romanov, A., Rooney, J., & Chen, W. (2008). Non-cytotoxic, in situ gelable hydrogels composed of N-carboxyethyl chitosan and oxidized dextran. *Biomaterials*, *29*(29), 3905-3913.

[173] Matrices, S. (1963). Mechanism of Sustained- Action Medication.

[174] Irma, A., Villegas, M., & Graciela, A. (2018). Validation of kinetic modeling of progesterone. *Asian Journal of Pharmaceutical Sciences*, *13*(1), 54–62. https://doi.org/10.1016/j.ajps.2017.08.007

[175] Dash, S., Murthy, P. N., Nath, L., & Chowdhury, P. (2010). Kinetic modeling on drug release from controlled drug delivery systems. *Acta Pol Pharm*, *67*(3), 217-23.

[176] Huang, X., & Brazel, C. S. (2001). On the importance and mechanisms of burst release in matrix-controlled drug delivery systems. Journal of controlled release, 73(2-3), 121-136.

[177] Place, E. S., Rojo, L., Gentleman, E., Sardinha, J. P., & Stevens, M. M. (2011). Strontium-and zinc-alginate hydrogels for bone tissue engineering. Tissue Engineering Part A, 17(21-22), 2713-2722.

[178] Song, Y., Gao, J., Xu, X., Zhao, H., Xue, R., Zhou, J., ... & Qiu, H. (2017). Fabrication of thermal sensitive folic acid based supramolecular hybrid gels for injectable drug release gels. Materials Science and Engineering: C, 75, 706-713.